1521-0111/12/8203-383–399$25.00
MOLECULAR PHARMACOLOGY
Copyright © 2012 The American Society for Pharmacology and Experimental Therapeutics
*Mol Pharmacol* 82:383–399, 2012

Vol. 82, No. 3
78352/3786717



# Carbonylation Induces Heterogeneity in Cardiac Ryanodine Receptor Function in Diabetes Mellitus

Chun Hong Shao, Chengju Tian, Shouqiang Ouyang, Caronda J. Moore, Fadhel Alomar, Ina Nemet, Alicia D'Souza, Ryoji Nagai, Shelby Kutty, George J. Rozanski, Sasanka Ramanadham, Jaipaul Singh, and Keshore R. Bidasee

*Departments of Pharmacology and Experimental Neuroscience (C.H.S., C.T., S.O., C.J.M., F.A., K.R.B.), Cellular and Integrative Physiology (G.J.R.), and Environmental, Occupational, and Agricultural Health (K.R.B.), University of Nebraska Medical Center, Omaha, Nebraska; Department of Pharmacology, University of Dammam, Dammam, Kingdom of Saudi Arabia (F.A.); Laboratory for Carbohydrate, Peptide, and Glycopeptide Research, Rudjer Boskovic Institute, Zagreb, Croatia (I.N.); School of Forensic and Investigative Science, University of Central Lancashire, Preston, United Kingdom (A.D., J.S.); Laboratory of Food and Regulation Biology, Department of Bioscience, School of Agriculture, Tokai University, Tokyo, Japan (R.N.); Joint Division of Pediatric Cardiology, University of Nebraska/Creighton University and Children's Hospital and Medical Center, Omaha, Nebraska (S.K.); Department of Physiology and Biophysics, University of Alabama, Birmingham, Alabama (S.R.); and Nebraska Center for Redox Biology, Lincoln, Nebraska (K.R.B.)*

Received February 20, 2012; accepted May 25, 2012

## ABSTRACT

Heart failure and arrhythmias occur at 3 to 5 times higher rates among individuals with diabetes mellitus, compared with age-matched, healthy individuals. Studies attribute these defects in part to alterations in the function of cardiac type 2 ryanodine receptors (RyR2s), the principal $Ca^{2+}$-release channels on the internal sarcoplasmic reticulum (SR). To date, mechanisms underlying RyR2 dysregulation in diabetes remain poorly defined. A rat model of type 1 diabetes, in combination with echocardiography, in vivo and ex vivo hemodynamic studies, confocal microscopy, Western blotting, mass spectrometry, site-directed mutagenesis, and [$^3$H]ryanodine binding, lipid bilayer, and transfection assays, was used to determine whether post-translational modification by reactive carbonyl species (RCS) represented a contributing cause. After 8 weeks of diabetes, spontaneous $Ca^{2+}$ release in ventricular myocytes increased ~5-fold. Evoked $Ca^{2+}$ release from the SR was nonuniform (dyssynchronous). Total RyR2 protein levels remained unchanged, but the ability to bind the $Ca^{2+}$-dependent ligand [$^3$H]ryanodine was significantly reduced. Western blotting and mass spectrometry revealed RCS adducts on select basic residues. Mutation of residues to delineate the physiochemical impact of carbonylation yielded channels with enhanced or reduced cytoplasmic $Ca^{2+}$ responsiveness. The prototype RCS methylglyoxal increased and then decreased the RyR2 open probability. Methylglyoxal also increased spontaneous $Ca^{2+}$ release and induced $Ca^{2+}$ waves in healthy myocytes. Treatment of diabetic rats with RCS scavengers normalized spontaneous and evoked $Ca^{2+}$ release from the SR, reduced carbonylation of RyR2s, and increased binding of [$^3$H]ryanodine to RyR2s. From these data, we conclude that post-translational modification by RCS contributes to the heterogeneity in RyR2 activity that is seen in experimental diabetes.

## Introduction

More than 350 million people throughout the world have diabetes mellitus, and ~70% of them develop a unique type of heart failure referred to as diabetic cardiomyopathy (http://www.diabetes.org/living-with-diabetes/complications; http://www.who.int/mediacentre/factsheets/fs312/en). A significant proportion of these individuals die prematurely as a result of fatal, stress-induced, ventricular arrhythmia (Bertoni et al., 2004)

This work was supported in part by the National Institutes of Health National Heart, Lung, and Blood Institute [Grant HL085061]; the Edna Ittner Research Foundation; the American Diabetes Association [Grant 1-06-RA-11]; and a grant-in-aid from the Ministry of Education, Science, Sports, and Culture of Japan [Grant 18790619].

C.H.S., C.T., and S.O. contributed equally to this work.

Article, publication date, and citation information can be found at http://molpharm.aspetjournals.org.

http://dx.doi.org/10.1124/mol.112.078352.

**ABBREVIATIONS:** SR, sarcoplasmic reticulum; RyR2, type 2 ryanodine receptor; DMEM, Dulbecco's modified Eagle's medium; RCS, reactive carbonyl species; ROS, reactive oxygen species; CHAPS, 3-[(3-cholamidopropyl)dimethylammonio]-1-propanesulfonic acid; MS, mass spectrometry; MS/MS, tandem mass spectrometry; TOF, time of flight; GA, glycolaldehyde; STZ, streptozotocin; MALDI, matrix-assisted laser desorption ionization; MGO, methylglyoxal; SERCA2, sarco(endo)plasmic reticulum $Ca^{2+}$-ATPase; Py, pyridoxamine; Ag, aminoguanidine; cRyR2, control type 2 ryanodine receptor; dRyR2, diabetic type 2 ryanodine receptor; Ins-DRyR2, insulin-treated diabetic type 2 ryanodine receptor.

(http://www.diabetes.org/living-with-diabetes/complications). Mechanisms responsible for the reduced basal and stress-induced aberrant ventricular contractions in individuals with diabetes mellitus remain incompletely defined, and therapeutic strategies to slow their development and progression are virtually nonexistent.

Efficient, rhythmic, ventricular contractions depend in part on adequate and synchronized release of $Ca^{2+}$ from the sarcoplasmic reticulum (SR) through type 2 ryanodine receptor (RyR2) $Ca^{2+}$-release channels. Alterations in RyR2 expression or function reduce the rate and amplitude of $Ca^{2+}$ release from the SR. Uncoordinated opening of RyR2s triggers delayed afterdepolarization and arrhythmias (Lehnart et al., 1998; Yano et al., 2009; Watanabe and Knollmann, 2011).

Studies reported either no change or reductions in steady-state levels of RyR2 protein in diabetes (Bidasee et al., 2001, 2003; Netticadan et al., 2001; Zhong et al., 2001; Belke et al., 2004; Yaras et al., 2005; Ligeti et al., 2006; Pereira et al., 2006). Increased spontaneous $Ca^{2+}$ release, which is characteristic of enhanced cellular RyR2 activity, was observed in ventricular myocytes isolated from rats with streptozotocin (STZ)-induced diabetes (Yaras et al., 2005; Shao et al., 2007). The latter was attributed in part to increased phosphorylation of RyR2 at Ser2808(9) and Ser2814(5), arising from enhanced protein kinase A and $Ca^{2+}$-calmodulin kinase II activities, and a reduction in the amount of the immunophilin FK506 binding protein 12.6 bound to RyR2 (Netticadan et al., 2001; Yaras et al., 2005; Shao et al., 2007, 2009). When RyR2s were isolated from diabetic rat hearts (dRyR2s), their ability to bind the $Ca^{2+}$-dependent ligand [$^3$H]ryanodine was significantly reduced, consistent with a reduction in activity (Bidasee et al., 2003; Shao et al., 2007). Electrically evoked $Ca^{2+}$ release from the SR was nonuniform (dyssynchronous) in diabetic myocytes (Shao et al., 2007), which suggests uncoupling between L-type $Ca^{2+}$ channels and RyR2s. These paradoxical findings led us to propose the existence of two populations of RyR2s in diabetic myocytes, one population with enhanced $Ca^{2+}$ responsiveness and one with reduced $Ca^{2+}$ responsiveness (i.e., heterogeneity in RyR2 function in diabetes) (Shao et al., 2007). We purified dRyR2s under reducing and dephosphorylating conditions and, by using lipid bilayers, identified a population of channels with enhanced responsiveness to $Ca^{2+}$, ATP, and cADP-ribose and reduced responsiveness to $Mg^{2+}$ (Tian et al., 2011). The population of RyR2s with reduced $Ca^{2+}$ responsiveness and the mechanisms responsible for heterogeneity in RyR2 function in diabetes remain to be characterized.

Reactive carbonyl species (RCS) are small electrophiles generated from glucose and fatty acid auto-oxidation, through polyol pathway flux, and by enzymes such as vascular adhesion protein-1/serum semicarbazide-sensitive amine oxidase (Baynes and Thorpe, 1999; Uchida, 2000; Ellis, 2007; Vander Jagt, 2008). At low micromolar concentrations, RCS regulate cell proliferation, prevent aggregation of proteins, and tag proteins for degradation (Nagaraj et al., 2003; Barrera et al., 2004; Dalle-Donne et al., 2006; Wong et al., 2010; Segré and Chiocca, 2011). In diabetes, production of RCS, including lipid-derived malondialdehyde and 4-hydroxynonenal and glucose-derived glyoxal, deoxyglucosone, and methylglyoxal (MGO), increases (Slatter et al., 2004; Lapolla et al., 2005; Fosmark et al., 2009; Vicentini et al., 2011). These electrophiles react with susceptible basic amino acids on proteins to form RCS adducts. To our knowledge, no enzymes that are capable of breaking RCS adducts after they are formed on proteins have been identified in mammalian cells. Therefore, RCS adducts formed on proteins with slow turnover, such as RyR2s ($t_{1/2} \sim 9$ days) (Ferrington et al., 1998), can be viewed as "diabetes-induced mutations."

By using matrix-assisted laser desorption ionization (MALDI)-time of flight (TOF)-mass spectrometry (MS) and a Perl script, we previously detected RCS adducts on RyR2s isolated from hearts of rats with STZ-induced diabetes (Bidasee et al., 2003). These adducts were not confirmed with other methods, however, and their impact on RyR2 function was not characterized. The hypothesis for the present study was that carbonylation (post-translational modification by RCS) is an underlying cause of the heterogeneity in RyR2 activity seen in diabetes.

## Materials and Methods

### Antibodies and Reagents

RyR2-specific antibodies were obtained from Thermo Fisher Scientific (Waltham, MA), and argpyrimidine-specific antibodies were from JaiCA (Zhizuoka, Japan). Antibodies to $N^{\varepsilon}$-carboxy(methyl)lysine, 3-deoxyglycosone/imidazolone, GA-pyridine, pentosidine, and pyrraline were supplied by Dr. Royji Nagai (Japan Women's University, Tokyo, Japan) and are now available through Cosmo Bio USA, Inc. (Carlsbad, CA). [$^3$H]Ryanodine was purchased from GE Healthcare (Chalfont St. Giles, Buckinghamshire, UK), phosphatidylserine, phosphatidylcholine, and phosphatidylethanolamine were obtained from Avanti Polar Lipids (Alabaster, AL), insulin pellets were obtained from LinShin Canada Inc. (Scarborough, Canada), and pyridoxamine and aminoguanidine were purchased from Sigma-Aldrich (St. Louis, MO). MitoSOX Red and MitoTracker Green were obtained from Invitrogen (Carlsbad, CA). MGO was synthesized, purified, and quantified in our laboratory, by using methods described previously (Nemet et al., 2004). All other reagents used were of the highest grade commercially available.

### Induction and Verification of Type 1 Diabetes

The procedures involving rats that were used in this study were approved by the institutional animal care and use committee of the University of Nebraska Medical Center and adhered to the *Guide for the Care and Use of Laboratory Animals* (Institute of Laboratory Animal Resources, 1996). The induction of diabetes with STZ and the care of rats with type 1 diabetes were described in detail previously (Shao et al., 2009; Tian et al., 2011).

### Treatment of Diabetic Animals

Two weeks after injection of STZ (in 0.1 M citrate buffer, pH 4.5), diabetic rats were randomly divided into three groups. One group was treated with pyridoxamine (Py) (1.6 g/kg per day) in drinking water for 5 to 6 weeks (Shao et al., 2011), the second group was treated with aminoguanidine (Ag) (1.6 g/kg per day) (Shao et al., 2010), and the third group remained untreated. Four weeks later, insulin pellets were implanted subcutaneously in some untreated diabetic animals, to attain the euglycemic state. Two weeks after injection of citrate buffer, control animals were divided into three groups. One group was treated with pyridoxamine (2.0 g/kg per day, because these rats drink one third less water than diabetic rats) for 5 to 6 weeks, the second group was treated with aminoguanidine (2.0 g/kg per day), and the third group remained untreated.

### Blood Parameters

Blood samples were collected from the left renal arteries after administration of anesthesia and were assayed for glucose, insulin,

thiobarbituric acid-reactive substances (primarily lipid-derived malondialdehyde), serum semicarbazide-sensitive amine oxidase activity, MGO (a glucose-derived RCS), and glycosylated hemoglobin, as described previously (Shao et al., 2010, 2011).

### Establishment of Diabetic Cardiomyopathy (Reduced Ventricular Function)

M-mode echocardiography was performed at the end of the 8-week protocol with anesthetized animals (100 mg/kg ketamine/2.5 mg/kg acepromazine i.p.), to confirm reduced left ventricular function (in vivo) and diabetic cardiomyopathy (Shao et al., 2010).

### Establishment of Stress-Induced Aberrant Ventricular Contractions

After euthanasia with thiobutabarbital (Inactin; 75 mg/kg i.p.), the chest cavities of control, diabetic, and insulin-treated diabetic animals were opened, and the hearts were removed, mounted on a Langendorff apparatus through the aortas, and perfused retrogradely with oxygenated Krebs-Henseleit buffer (118 mM NaCl, 27.2 mM $NaHCO_3$, 4.8 mM KCl, 1.2 mM $MgSO_4$, 1.0 mM $KH_2PO_4$, 1.25 mM $CaCl_2$, 11 mM glucose, 37°C). A silk thread was inserted through the apex of each ventricle and attached to a force displacement transducer (FT03C; Grass Instruments, Quincy, MA) for measurement of developed ventricular tension (contraction). After stabilization, the right atrium of each heart was excised, the atrioventricular node was crushed, and a pair of platinum electrodes was inserted into the left ventricular wall, to pace the ventricle at 180 to 200 beats/min. Basal ventricular tension was determined; isoproterenol (1 ml of a 1 nM solution) was then injected through a side arm, and changes in ventricular tension were determined. Hearts were allowed to stabilize for 30 min, a higher dose of isoproterenol (1 ml of a 10 nM solution) was injected, and changes in developed ventricular tension were determined.

### Dyad Junction Architecture

Hearts were perfused retrogradely with Krebs-Henseleit buffer on a Langendorff apparatus, to remove blood, and then were fixed with 3.5% glutaraldehyde in 1% phosphate-buffered saline, pH 7.2. Left ventricles were cut into pieces, washed three times with 0.1 M Sorenson's phosphate-buffered saline, pH 7.3, postfixed in 1% aqueous osmium tetroxide solution for 1 h at room temperature, and washed three times with Sorenson's phosphate-buffered saline. Tissues were dehydrated in graded ethanol (50, 70, 90, 95, and 100% three times), followed by three times with 100% propylene oxide, and then were left overnight in a 1:1 mixture of propylene oxide and Araldite embedding medium (Polysciences, Warrington, PA). Ventricular sections were placed in flat silicon rubber molds with fresh Araldite and were polymerized overnight at 65°C. Ultrathin sections (~30–40 nm) were prepared with a Leica EM-UC 6 microtome (Leica Microsystems, Inc., Bannockburn, IL) with a Diatome diamond knife (Diatome, Biel, Switzerland) and were stained with 2% uranyl acetate and Reynold's lead citrate. A transmission electron microscope [Philips 410LS (FEI, Hillsboro, OR), operating at 80 kV] was used to assess dyad junction architecture and the distance between T-tubules and junctional SR in a random manner.

### Myocyte Isolation and Confirmation of Altered SR $Ca^{2+}$ Release

Ventricular myocytes were isolated through retrograde collagenase perfusion, as described previously (Mitra and Morad, 1985; Shao et al., 2007). Confocal microscopy (whole-cell and line-scan modes) was used to assess spontaneous and evoked $Ca^{2+}$ release in ventricular myocytes (Shao et al., 2007). Caffeine-induced $Ca^{2+}$ transient amplitudes were measured and used as indices of SR $Ca^{2+}$ contents (Shao et al., 2009).

### Confirmation and Determination of Location of Carbonyl Adducts on RyR2s

**Western Blotting.** Western blots with membrane vesicles (30 $\mu$g) were used to determine relative levels of RyR2 protein in hearts from control, diabetic, insulin-treated, and drug-treated animals (Shao et al., 2011; Tian et al., 2011). Western blots with junctional sarcoplasmic reticulum vesicles (60 $\mu$g), which were prepared by fractionating membrane vesicles on discontinuous sucrose gradients (Tian et al., 2011), were used to determine relative levels of argpyrimidine, $N^{\varepsilon}$-carboxy(methyl)lysine, 3-deoxyglycosone/hydroimidazolone, GA-pyridine, pentosidine, and pyrraline adducts with well characterized antibodies (Ling et al., 1998; Oya et al., 1999; Nagai et al., 2003, 2008). $\beta$-Actin served as the internal control, to correct for variations in sample loading.

**Mass Spectrometry.** Immunoprecipitated RyR2s were solubilized in gel dissociation medium and subjected to electrophoresis on 4 to 15% denaturing SDS-polyacrylamide gels (prerun for 10 min before sample loading) for 180 min at 150 V. Gels were stained with Coomassie Blue and destained with 30% methanol, and RyR2 bands were excised, digested with trypsin, desalted with ZipTips (Millipore Corp., Billerica, MA), and divided into two aliquots. One aliquot was subjected to MALDI-TOF-MS, and data were searched for peptides with RCS adducts (Bidasee et al., 2003). The other aliquot was subjected to liquid chromatography-MS/MS with electrospray ionization (in a nanospray configuration) with a microcapillary RP-$C_{18}$ column (New Objectives, Woburn, MA), to determine peptide sequences containing RCS adducts. MS/MS was performed with an ion trap mass spectrometer (LCQ-Deca XP Plus; Thermo Fisher Scientific). Data-dependent acquisition was performed with a 1-s survey scan between 380 and 1900 atomic mass units, followed by a 2.4-s MS/MS data acquisition between 200 and 1300 atomic mass units. Mascot Wizard was obtained from Matrix Science Inc. (Boston, MA).

### Site-Directed Mutagenesis

To delineate the physiochemical effects of carbonylation, mutation studies (with single and double mutations) involving five amino acid residues [i.e., Arg1611 (between regions 1 and 2), Lys2190 and Lys2888 (within the middle region), and Arg4462 and Arg4683 (within the C-terminal region)] were performed. Mouse RyR2 cDNA (a gift from Dr. Wayne Chen, University of Alberta, Edmonton, Alberta, Canada) was excised from pcDNA3.0 with NheI and NotI, purified through agarose gel electrophoresis, and digested with BsiWI, which yielded two fragments, a NheI/BsiWI fragment (bases 0–8864; fragment 1) and a BsiWI/NotI fragment (bases 8865–14,904; fragment 2). Fragments were cloned in-frame into pGEM-3z by using their respective restriction sites, which yielded clone 1 (bases 0–8864) and clone 2 (bases 8865–14,904), respectively. QuikChange mutagenesis kits (Agilent Technologies, Santa Clara, CA) were used to mutate Arg1611, Lys2190, and Lys2888 (Lys2887 in mouse cDNA) in clone 1 and Arg4462 and Arg4683 (Arg4682 in mouse cDNA) in clone 2 to tyrosines and tryptophans. These residues were selected because they best reflected the charge neutralization and increase in bulk induced by RCS adducts. Glycine mutants were also created, to assess the impact of charge neutralization only. Oligonucleotide primers of ~40 base pairs were used. After mutation, plasmids were transformed into competent HB101 cells, amplified in liquid cultures, and purified with MaxiPrep columns (QIAGEN, Valencia, CA), and mutations were confirmed through oligonucleotide sequencing. The fragments containing mutations were excised from pGEM-3z with appropriate restriction enzymes, purified through agarose gel electrophoresis, and ligated to the nonmutated fragment with T4 ligase (Promega, Madison, WI), to create full-length RyR2s containing mutations. Forward and reverse oligonucleotide sequencing was performed (mutation site and four or five randomly chosen sites) to ensure that nonspecific mutations did not occur during the procedures. Wild-type and mutant RyR2 cDNAs were then cloned in-frame into pCMS-EGFP

(Clontech, Mountain View, CA) by using the NheI and NotI restriction sites, transformed into competent HB101 cells, amplified in liquid broth, and purified with plasmid MaxiPrep columns (QIAGEN).

### Expression of Wild-Type and Mutated RyR2s

Wild-type and mutated RyR cDNAs (15–20 $\mu$g) were transfected into HEK-293T cells grown in Dulbecco's modified Eagle's medium (DMEM) with 1.8 mM $Ca^{2+}$ [passage 10 or higher, 30–40% confluence, 18–20 dishes (100 mm)], by using calcium phosphate (Chen and Okayama, 1987). These cells were chosen because they express little or no RyR2 (Luo et al., 2005). The medium was changed 6 to 8 h after transfection, and cells were allowed to grow for an additional 36 to 38 h. After that time, cells were washed with 1× phosphate-buffered saline containing 1 mM EDTA, harvested through centrifugation (500*g* for 3 min), resuspended in buffer containing 0.25 M sucrose, and 10 mM histidine, pH 7.3, and a protease inhibitor mixture (1 mM benzamidine, 2 $\mu$g/ml leupeptin, 2 $\mu$g/ml pepstatin A, 2 $\mu$g/ml aprotinin, and 0.5 mM phenylmethylsulfonyl fluoride), and homogenized with a Polytron homogenizer (5 × 6 s, setting 5; Kinematica, Basel, Switzerland). Homogenates were centrifuged (85,195*g* for 45 min), and membranes were collected, quick-frozen in liquid nitrogen, and stored at −80°C. Serial-dilution Western blotting was performed to determine RyR2 protein contents in membrane vesicles.

### Preparation of Proteoliposomes Containing RyR2s

Proteoliposomes containing wild-type or mutated RyR2s were prepared as described previously (Tian et al., 2011), except that HEK-293T membranes at 3.0 mg/ml were solubilized with 1.5% 3-[(3-cholamidopropyl)dimethylammonio]-1-propanesulfonicacid (CHAPS). Proteoliposomes containing wild-type and mutant RyR2s were stored in the vapor phase of liquid nitrogen until use.

### Cytoplasmic $Ca^{2+}$ Responsiveness of Wild-Type and Mutated RyR2s

**[$^3$H]Ryanodine Binding Assays.** Membrane vesicles (0.1 mg/ml) were incubated in binding buffer (500 mM KCl, 20 mM Tris-HCl, 2 mM GSH, 100 $\mu$M EGTA, and 6.7 nM [$^3$H]ryanodine, pH 7.4) with varying $Ca^{2+}$ concentrations (0–4 mM) for 2 h at 37°C. After incubation, membranes were filtered and washed, and the amount of [$^3$H]ryanodine bound to RyR2s was determined through liquid scintillation counting. Nonspecific binding was determined simultaneously by incubating vesicles with 1 $\mu$M unlabeled ryanodine (Shao et al., 2007).

**Planar Lipid Bilayer Assays.** These studies were conducted as described previously (Tian et al., 2011). After fusion of RyR2s to the lipid bilayer, $Ca^{2+}$ was added to the cis chamber and stirred vigorously for ~30 s. Channel activity (open probability, gating, and conductance) was recorded for 6 min (3 min at +35 mV and 3 min at −35 mV). Electrical signals were filtered at 2 kHz, digitized at 10 kHz, and analyzed by using pClamp (Molecular Devices, Sunnyvale, CA). All experiments were performed at room temperature (23–25°C) in ambient air.

**Transfection of Wild-Type and Mutated RyR2s into HEK-293T Cells and Responsiveness of Cells to Extracellular $Ca^{2+}$.** Wild-type RyR2, K2887W (a mutant with enhanced cis $Ca^{2+}$ responsiveness), R4462Y (a mutant with reduced cis $Ca^{2+}$ responsiveness), or a blank vector (pCMS-EGFP) was transfected into HEK-293T cells grown in DMEM by using calcium phosphate (Chen and Okayama, 1987). The medium was changed 6 to 8 h after transfection, and cells were allowed to grow for an additional 36 to 38 h. Cells were then washed, loaded with fura-2/acetoxymethyl ester (5 $\mu$M) in low-$Ca^{2+}$ Tyrode's solution (140 mM NaCl, 5.4 mM KCl, 1 mM $Na_2HPO_4$, 10 mM HEPES, 5 mM glucose, 1 mM $MgCl_2$, and 0.2 mM $Ca^{2+}$, pH 7.4) for 30 min at 37°C, placed on the stage of a Nikon TE2000 microscope (Nikon, Tokyo, Japan), and perfused with low-$Ca^{2+}$ Tyrode's solution at a rate of 1.0 ml/min. The $Ca^{2+}$ concentration in the perfusate was increased gradually (0.4, 0.6, 1.0, and 1.8 mM, 2.5 min each), and changes in cellular $Ca^{2+}$ levels were recorded. Caffeine (10 mM) was added at the end of the procedure, to confirm the presence of functional RyR2s in the cells assayed. Recordings were performed with a dual-excitation fluorescence photomultiplier system (Image Master fluorescence microscope; Photon Technology International, Lawrenceville, NJ), by using FELIX software (Photon Technology International). Cells were excited at 340 and 380 nm, and emission was measured at 510 nm.

### Assessment of Effects of MGO on RyR2 Activity

**[$^3$H]Ryanodine Binding Assays.** Experiments were conducted as described above except that varying levels of MGO (0–600 $\mu$M) were added to the binding buffer during incubation. In some experiments, membrane vesicles (0.1 mg/ml) were preincubated with varying amounts of MGO (0–400 $\mu$M) in binding buffer (500 mM KCl, 20 mM Tris-HCl, and 13 $\mu$M $Ca^{2+}$, pH 7.4) at 37°C for 30 min. After that time, membranes were divded into 10 tubes, 6.7 nM [$^3$H]ryanodine and increasing amounts of $Ca^{2+}$ (0–4 mM) were added, and incubation was continued at 37°C for 1.5 h. Membranes were filtered and washed, and the amount of [$^3$H]ryanodine bound was used as an index of the ability of MGO to modulate RyR2 activity.

**Lipid Bilayer Assays.** Purified RyR2s from control animals were incorporated into the lipid bilayer with cis $Ca^{2+}$ levels of 3.3 $\mu$M. MGO (0–80 $\mu$M) was added to the cis chamber and stirred vigorously for 30 s. Channel activity (open probability, gating, and conductance) was recorded for 6 min (3 min at +35 mV and 3 min at −35 mV).

**Spontaneous and Evoked $Ca^{2+}$ Release in Myocytes.** Ventricular myocytes isolated from control rats in DMEM/F12 medium with 1.8 mM $CaCl_2$ were loaded with fluo-3/acetoxymethyl ester for 30 min at 37°C. Cells were then washed, medium was replaced with Tyrode's solution (140 mM NaCl, 5.4 mM KCl, 1 mM $Na_2HPO_4$, 10 mM HEPES, 5 mM glucose, 1.0 mM $Ca^{2+}$, and 1 mM $MgCl_2$, pH 7.4), and chambers containing fluo-3-loaded cells were placed on the stage of a laser confocal microscope [Nikon swept-field confocal microscope equipped with a Cascade 512B high-quantum efficiency digital camera (Photometrics, Tucson, AZ), an argon-krypton laser (5% intensity), and a 60× plan apochromatic lens]. Images of cells were collected every 2 s (3 ms per scan) for 3 min, to determine basal spontaneous $Ca^{2+}$ release. MGO (25 $\mu$M) was then added, and spontaneous $Ca^{2+}$ release was assayed over 5 min. Experiments were also performed in line-scan mode by using a Zeiss 410 confocal microscope (Carl Zeiss Inc., Thornwood, NY) and field-stimulating cells at 0.25 Hz (10 V for 10 ms), as described previously (Shao et al., 2009). Caffeine (10 mM) was added 6 min after the addition of MGO, to assess SR $Ca^{2+}$ contents.

### Effects of MGO on Mitochondrial Production of Superoxide and Total Reactive Oxygen Species

Rat ventricular myocytes in DMEM/F12 medium with 1.8 mM $CaCl_2$ were loaded with the mitochondria-localizing probe MitoTracker Green (100 nM), followed by the fluorogenic, mitochondria-targeted, superoxide/reactive oxygen species (ROS) probe MitoSOX Red (2 $\mu$M), for 15 min each. After loading, DMEM was replaced with Tyrode's solution (140 mM NaCl, 5.4 mM KCl, 1 mM $Na_2HPO_4$, 10 mM HEPES, 5 mM glucose, 1.0 mM $Ca^{2+}$, and 1 mM $MgCl_2$, pH 7.4), and cells were placed on the stage of a Zeiss LSM 510 Meta laser scanning microscope, with excitation at 405 nm (to detect the superoxide-specific 2-hydroxyethidium product of oxidized MitoSOX Red) and 488 nm (to detect ROS-produced ethidium products) to capture fluorescence images for MitoTracker Green and MitoSOX Red, respectively. MitoTracker Green was excited at 488 nm, and emissions were monitored at 516 nm. MitoSOX Red fluorescence was quantified with ImageJ analysis software (http://rsbweb.nih.gov/ij/).

### Statistical Analyses

Differences among values for the groups (control, diabetic, insulin-treated diabetic, Py-treated control, Py-treated diabetic, Ag-treated

control, Ag-treated diabetic, and wild-type and mutant RyR2 groups) were evaluated through analysis of variance with GraphPad Prism (GraphPad Software Inc., San Diego, CA). Data shown are mean ± S.E.M. values. Results were considered significantly different at $p < 0.05$ (95% confidence interval).

## Results

### General Characteristics of Animals Used in Study

General characteristics of the animals used in the study are shown in Table 1. M-mode echocardiography confirmed reductions in ejection fraction and fractional shortening in diabetic animals. Insulin treatment reversed these changes, which indicated that the changes in ejection fraction and fractional shortening resulted from the diabetes and not the diabetogenic agent STZ. Py and Ag treatments also blunted reductions in ejection fraction and fractional shortening. Insulin and Ag treatments blunted the increase in serum thiobarbituric acid-reactive substance (malondialdehyde) levels, whereas insulin, Py, and Ag treatments blunted the increase in serum semicarbazide-sensitive amine oxidase activity induced by diabetes.

### Ex Vivo Stress-Induced Aberrant Ventricular Contractions

Maximal developed tension (i.e., extent of contraction) values for ex vivo diabetic hearts were 22.5 ± 3.5% less than those for control hearts (Fig. 1i). Values for contractions induced by isoproterenol (1 and 10 nM) also were significantly lower for diabetic rat hearts ($p < 0.05$). Treatment of diabetic animals with insulin for 2 weeks blunted these changes, which emphasized that reductions in ventricular contractions stemmed from the diabetes and not the diabetogenic agent STZ. When challenged with 10 nM isoproterenol, 56% of diabetic rat hearts (9 of 16 hearts) exhibited abnormal ventricular contractions, compared with 13% of control hearts (2 of 15 hearts; $p < 0.05$) (Fig. 1ii). In five of those nine diabetic hearts, normal contractions resumed within 10 to 30 s after injection of 10 nM isoproterenol (Fig. 1ii). In the other four diabetic hearts, rhythmic contractions ceased. Three (21%) of 14 hearts from insulin-treated diabetic rats exhibited abnormal contractions when challenged with 10 nM isoproterenol. Two of 16 diabetic hearts, 1 of 15 control hearts, and 1 of 14 insulin-treated diabetic hearts tested exhibited abnormal contractions in response to 1 nM isoproterenol ($p > 0.05$). These data are consistent with the notion that diabetic hearts are more likely to exhibit abnormal contractions when stressed (Bertoni et al., 2004) (http://www.diabetes.org/living-with-diabetes/complications).

### Altered SR $Ca^{2+}$ Release in Diabetic Myocytes

**Spontaneous $Ca^{2+}$ Release ($Ca^{2+}$ Sparks).** Myocytes from the hearts of diabetic animals exhibited a 4.8-fold higher frequency of spontaneous $Ca^{2+}$ release from the SR, compared with myocytes from control heart1s (13.6 ± 1.2 versus 2.8 ± 0.5 sparks/s in 50 μm; $p < 0.05$, ≥32 cells (Fig. 2i). There was no difference in the full-width-at-half-maximum values for sparks from control and diabetic myocytes (2.05 ± 0.02 and 2.10 ± 0.04 μm, respectively; 200 sparks from each group). Insulin treatment blunted the increase in $Ca^{2+}$ spark frequency, which indicated that this defect stemmed from the diabetes and not from the diabetogenic agent STZ. These data confirmed earlier studies that showed increased cellular activity of RyR2s in diabetic myocytes (Yaras et al., 2005; Shao et al., 2007).

**Evoked $Ca^{2+}$ Release.** When cells were field-stimulated at 0.5 Hz, the rate of evoked $Ca^{2+}$ release from the SR and the $Ca^{2+}$ transient amplitude were reduced in diabetic myocytes, compared with control myocytes (78.2 ± 8.1 versus 108.2 ± 5.2 arbitrary fluorescence units/s and 3.3 ± 0.4 versus 4.8 ± 0.1 arbitrary fluorescence units, respectively) (Fig. 2ii). The $Ca^{2+}$ decay time was significantly increased in diabetic myocytes, compared with control myocytes (722.1 ± 14.5 versus 260.5 ± 8.1 ms). Evoked $Ca^{2+}$ release from the SR was dyssynchronous (nonuniform) in more than 50% of myocytes from diabetic animals, with diastolic $Ca^{2+}$ release between pulses; approximately 9% of diabetic myocytes exhibited $Ca^{2+}$ alternans (Fig. 2ii). These data confirmed nonuniform evoked release of $Ca^{2+}$ from the SR (Shao et al., 2007).

### Dyad Junction Architecture

Evoked $Ca^{2+}$ release from the SR is dependent on the ability of L-type $Ca^{2+}$ channels to respond to a depolarizing impulse, the spatial distance between T-tubules and SR membranes, and the responsiveness of RyR2s to $Ca^{2+}$ influx. A majority of studies reported no change in L-type $Ca^{2+}$ channel activity in myocytes from rats with STZ-induced diabetes (Jourdon and Feuvray, 1993; Choi et al., 2002;

TABLE 1
General characteristics of animals used in study

| Parameter | Control ($n = 48$) | Diabetic ($n = 48$) | Insulin-Treated Diabetic ($n = 48$) | Py-Treated Control ($n = 14$) | Py-Treated Diabetic ($n = 15$) | Ag-Treated Control ($n = 15$) | Ag-Treated Diabetic ($n = 15$) |
|---|---|---|---|---|---|---|---|
| Body mass, g | 370.0 ± 13.3 | 290.1 ± 17.3* | 324.0 ± 7.5 | 397.6 ± 12.9 | 283.5 ± 12.6 | 403.3 ± 7.8 | 304 ± 10.1 |
| Blood glucose level, mM | 5.0 ± 0.5 | 21.1 ± 1.4* | 8.1 ± 2.1** | 4.9 ± 1.1 | 20.1 ± 1.6 | 8.10 ± 0.33 | 22.02 ± 2.12 |
| Heart rate, beats/min | 370.2 ± 10.2 | 283.9 ± 13.2* | 327.5 ± 7.5** | 307 ± 20.6 | 282.1 ± 29.0 | 417.0 ± 19.8 | 294.1 ± 30.2 |
| Fractional shortening, % | 60.9 ± 3.2 | 49.3 ± 1.0* | 56.3 ± 2.6** | 58.9 ± 3.1 | 57.4 ± 3.7** | 57.9 ± 1.9 | 56.4 ± 3.7** |
| Ejection fraction, % | 83.5 ± 2.2 | 72.5 ± 1.0* | 80.3 ± 3.5** | 84.4 ± 5.2 | 81.5 ± 3.9** | 81.8 ± 2.9 | 80.1 ± .3.5** |
| Glycosylated hemoglobin, % | 4.1 ± 0.1 | 7.2 ± 0.1* | 4.7 ± 0.2** | 4.2 ± 0.2 | 7.6 ± 0.3 | 4.23 ± 0.21 | 8.2 ± 0.17 |
| Serum insulin level, ng/ml | 1.02 ± 0.21 | 0.31 ± 0.03* | 0.91 ± 0.02** | 1.10 ± 0.07 | 0.28 ± 0.04 | 0.67 ± 0.07 | 0.31 ± 0.03 |
| Serum TBARS level, nmol/ml | 2.4 ± 0.3 | 11.1 ± 1.9* | 4.1 ± 1.0** | 1.0 ± 0.2 | 8.0 ± 0.9 | 4.1 ± 0.9 | 7.2 ± 0.7** |
| Serum SSAO activity, units · $ml^{-1}$ · $min^{-1}$ | 0.32 ± 0.02 | 0.56 ± 0.03* | 0.35 ± 0.06** | 0.22 ± 0.01 | 0.39 ± 0.02** | 0.47 ± 0.03* | 0.41 ± 0.05** |
| Ventricular MGO level, μmol/100 mg tissue ($n = 6$) | 1.8 ± 0.2 | 4.2 ± 0.6* | 2.2 ± 0.4** | N.D. | N.D. | N.D. | N.D. |

TBARS, thiobarbituric acid-reactive substances; SSAO, semicarbazide-sensitive amine oxidase; N.D., not done.
* Significantly different from control value ($p < 0.05$).
** Significantly different from diabetic value ($p < 0.05$).

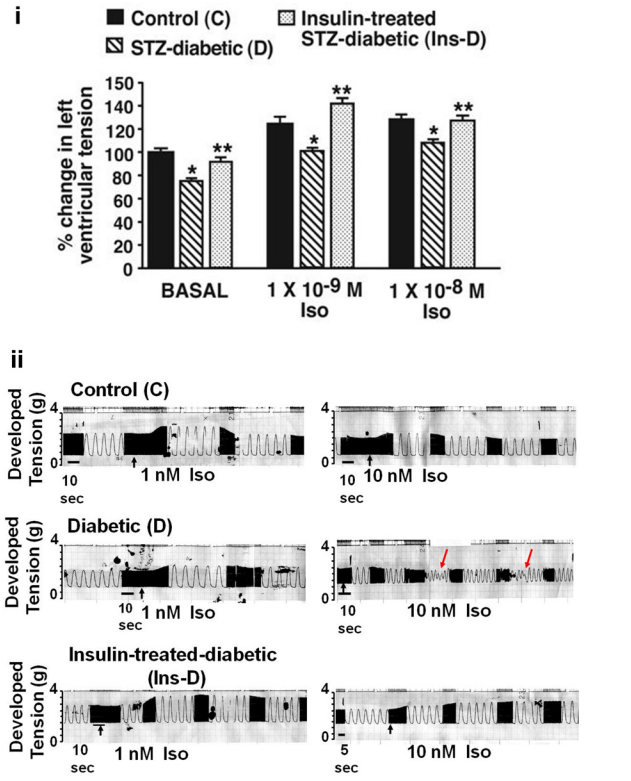


**Fig. 1.** Ex vivo ventricular function. i, basal and isoproterenol (Iso)-induced changes in left ventricular tension in ex vivo hearts from control, diabetic, and insulin-treated diabetic animals. Values shown are for ≥14 hearts. *, significantly different from control hearts ($p < 0.05$). **, significantly different from diabetic hearts ($p < 0.05$). ii, representative original tracings of left ventricular responses of hearts from control, diabetic, and insulin-treated diabetic animals challenged with 1 and 10 nM isoproterenol. Red arrows, abnormal ventricular contractions.

Bracken et al., 2006; Shao et al., 2007). This prompted us to ascertain whether the spatial distance between T-tubules and SR membranes (i.e., the dyad junction architecture) was altered in myocytes from rats with STZ-induced diabetes. Images collected randomly from the top, middle, and apex of ventricles from control, diabetic, and insulin-treated diabetic animals showed no significant difference in the distance between T-tubules and SR membranes (Fig. 2iii). The mean distance between SR and T-tubule membranes was 18.2 ± 4.8 nm in control rats (103 images from four rats), 16.2 ± 3.4 nm in diabetic rats (122 images from five rats), and 17.7 ± 5.4 nm in insulin-treated diabetic rats (81 images from four rats). These data indicated that the dyad junction architecture was not altered in myocytes from rats after 8 weeks of STZ-induced diabetes.

## Reduced RyR2 Activity in Diabetes

With no changes in the activity of L-type $Ca^{2+}$ channels and dyad junction architecture, we focused our attention on RyR2s. In this study, steady-state levels of RyR2 protein did not change after 8 weeks of diabetes but, at equivalent amounts, dRyR2s bound ~30% less [$^3$H]ryanodine than did cRyR2s at optimal $Ca^{2+}$ levels (530.2 ± 12.3 fmol of [$^3$H]ryanodine/mg of diabetic membranes, compared with 762.2 ± 13.6 fmol of [$^3$H]ryanodine/mg of control membranes; $p < 0.05$) (Fig. 3i). Treatment with insulin blunted the reduction in [$^3$H]ryanodine binding to RyR2s, which confirmed that this defect stemmed from diabetes and not from STZ. cRyR2s, dRyR2s, and RyR2s from insulin-treated animals (Ins-DRyR2s) exhibited similar affinities for the prototype ligand ryanodine (cRyR2, $K_d$ = 1.0 ± 0.1 nM; dRyR2, $K_d$ = 0.8 ± 0.1 nM; Ins-DRyR2, $K_d$ = 0.9 ± 0.1 nM; $p > 0.05$).

## Increased Carbonylation of RyR2s in Diabetes

Compared with cRyR2s, dRyR2s contained >2.5 times more immunoreactive $N^{\varepsilon}$-carboxy(methyl)lysine pyrraline, pentosidine, argpyrimidine, and deoxyglucosone/hydroimidazole adducts (Fig. 3, ii and iii). Immunoreactive GA-pyridine was found on dRyR2s but was not detected on cRyR2s. Insu-

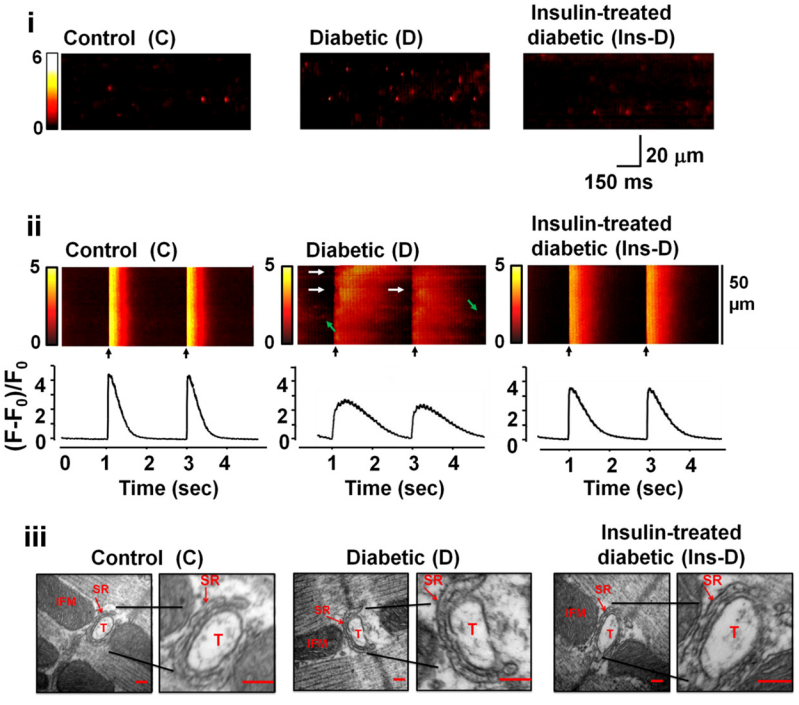


**Fig. 2.** Alterations in RyR2 activity in diabetic myocytes. i, representative line-scan images of spontaneous $Ca^{2+}$ release ($Ca^{2+}$ sparks) in myocytes from control, diabetic, and insulin-treated diabetic animals. ii, representative evoked $Ca^{2+}$ transients from control, diabetic, and insulin-treated diabetic myocytes with 0.5-Hz stimulation. iii, representative electron-microscopic images of dyad junctions from control, diabetic, and insulin-treated diabetic animals. IFM, interfibrillar mitochondrion; T, T-tubule. Scale bars, 100 nm.

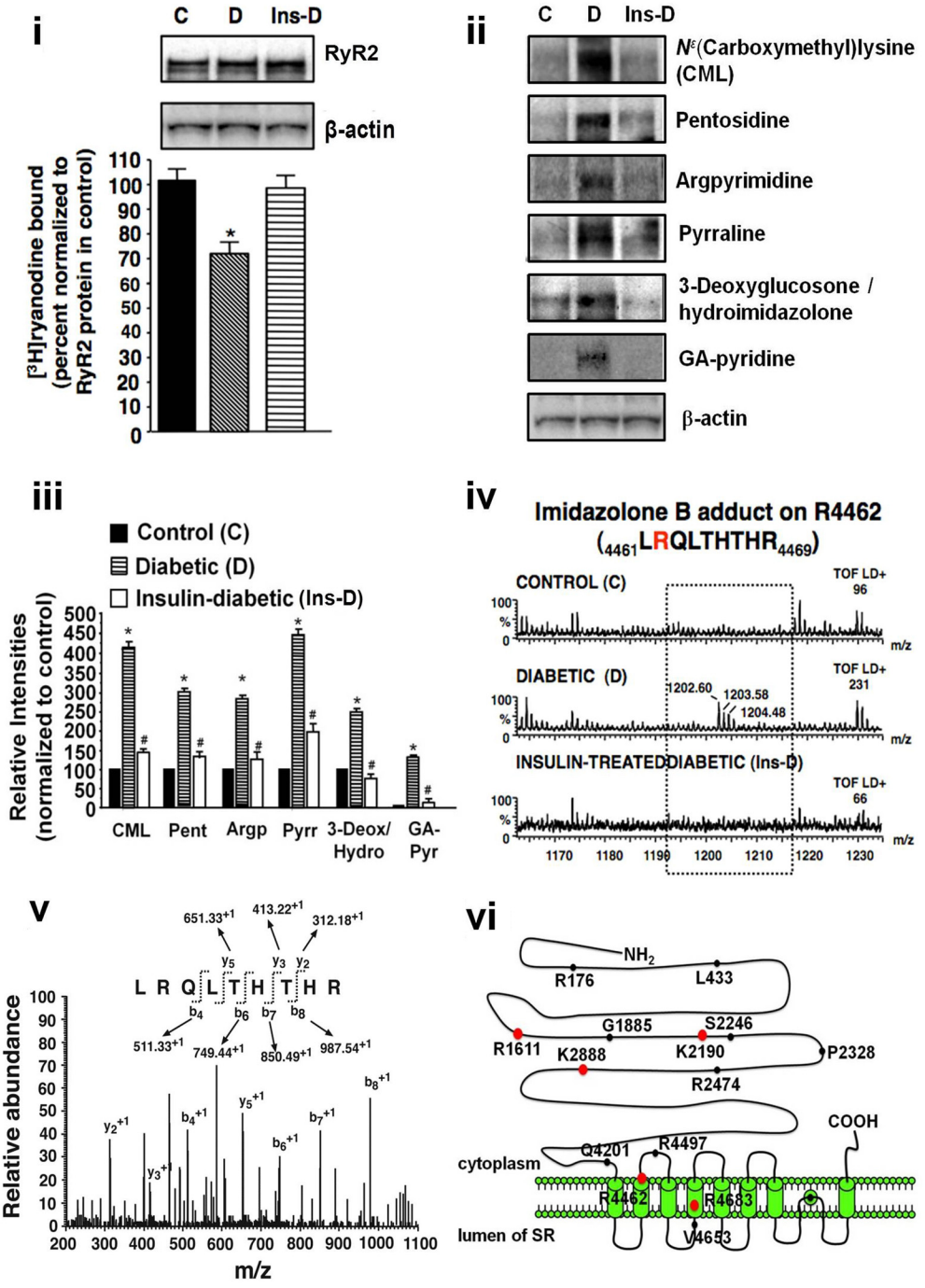


**Fig. 3.** Post-translational modification of RyR2 by reactive carbonyl species in diabetes. i, top, representative autoradiograms showing steady-state levels of RyR2 protein in membrane vesicles isolated from control (C), diabetic (D), and insulin-treated diabetic (Ins-D) rat hearts; bottom, graph showing normalized [$^3$H]ryanodine binding (mean ± S.E.M. of more than four experiments). *, significantly different from control value. ii, representative autoradiograms showing carbonyl adducts on RyR2s from control, diabetic, and insulin-treated diabetic rat hearts. Immunoblots were obtained by using 60 $\mu$g of membrane vesicles and using antibodies to $N^{\varepsilon}$-carboxy(methyl)lysine, argpyrimidine, 3-deoxyglucosone/hydroimidazolone, GA-pyridine, pentosidine, and pyrraline as the primary antibodies in Western blot assays (1:1000, for 16 h). iii, relative levels (mean ± S.E.M.) of carbonyl adducts on RyR2s in hearts from control, diabetic, and insulin-treated diabetic animals. Values shown are from four separate preparations. CML, $N^{\varepsilon}$-carboxy(methyl)lysine; Argp, argpyrimidine; 3-Deox/Hydro, 3-deoxyglycosone/hydroimidazolone; GA-Pyr, GA-pyridine; Pent, pentosidine; Pyrr, pyrraline. *, significantly different from control value; #, significantly different from diabetic value ($p < 0.05$). iv, alignment of MALDI-TOF mass spectra obtained after trypsin digestion of RyR2s from control, diabetic, and insulin-treated diabetic rats. An M+1 peak was present at 1202.60 Da in diabetic samples but not in the other samples. The Perl algorithm suggested that this peak was imidazolone B on Arg4462 ($_{4461}$LRQLTHTHR$_{4469}$). v, y and b ions obtained after fragmentation of the 1202.60-Da M+1 mass peak. vi, RyR2 structure. Red circles, locations of carbonyl adducts on RyR2; black circles, positions of other amino acids, for reference.

lin treatment blunted the levels of carbonyl adducts formed on RyR2s.

Digestion of cRyR2s, dRyR2s, and Ins-DRyR2s with trypsin yielded 302, 251, and 281 peptides, respectively, with $M+H^+$ values between 500 and 3000 Da. These peptides were within 10 ppm of theoretical RyR2 peptide values and covered ~65% of the primary sequence. The Perl script designed to compare experimental masses with theoretical digest masses (with up to three miscleaved peptides) and to search for modified peptides generated a list of five peptides with RCS adducts on lysine or arginine residues. Fragmentation of these peptides with tandem mass spectrometry confirmed that they originated from RyR2s. As an example, a single charged ion with *m/z* 1202.60 was found after digestion of dRyR2s but not cRyR2s or Ins-DRyR2s (Fig. 3iv). The Perl script predicted that this mass was derived from glyoxal/methylglyoxal-derived hydroimidazolone on Arg4462 in peptide $_{4461}$LRQLTHTHR$_{4469}$. Fragmentation of this peptide with tandem mass spectrometry afforded b and y M+1 ions that confirmed the peptide $_{4461}$LRQLTHTHR$_{4469}$ (Fig. 3v). We did not detect the imidazolone B adduct (142 Da) because it was below the set mass detection threshold. Because arginine is the only basic residue on this peptide at which an imidazolone adduct can be formed, we reason that imidazolone B is on Arg4462. The combination of MALDI-TOF-MS, Perl script, and MS/MS confirmed the locations of imidazolone B on Arg1611 (in $_{1607}$VDVSRISER$_{1615}$) and pyrraline adducts on Lys2190 (in $_{2185}$EITFPKMVANCCR$_{2197}$) and

Lys2888 (in $_{2887}$EKAQDILK$_{2892}$) in rat RyR2s. Arg4683 (in $_{4675}$AALDFSDAREK$_{4685}$) was modified with argpyrimidine in two experiments and with hydroimizazolone in two other experiments. The carbonylation sites on RyR2s were similar to those in our previous study (Bidasee et al., 2003), but the adduct type was different for some residues.

### Functional Impact of Carbonylation

**Rationale.** We next set out to determine whether RCS adducts were responsible for the functional heterogeneity of RyR2s seen in experimental type 1 diabetes mellitus. To date, chemical methods to insert a specific adduct at a defined amino acid residue without disrupting the tertiary structure of RyR2 are unavailable. Because carbonyl adducts neutralize basic charges and increase bulk, we reasoned that mutation of these residues to tyrosines, tryptophans, and glycines might provide insights into the roles these residues play in the overall function of RyR2 and might facilitate determination of the impact of carbonylation of these residues on RyR2 function. Three approaches were used to assess the activity of RyR2 mutants.

**$Ca^{2+}$-Dependent Binding of [$^3$H]Ryanodine.** Neutralizing the basic charge on Arg1611 by converting it to glycine did not significantly alter $Ca^{2+}$-dependent binding of [$^3$H]ryanodine to RyR2s (Fig. 4i). Neutralizing the basic charge and increasing the bulk at Arg1611 by converting it to tryptophan or tyrosine also did not alter the binding of [$^3$H]ryanodine (Fig. 4i). Neutralizing basic charges on Lys2190 or Lys2887 (the mouse equivalent of Lys2888) by converting each to glycine did not alter $Ca^{2+}$-dependent binding of [$^3$H]ryanodine (Fig. 4, ii and iii). However, neutralizing the basic charge and increasing the bulk at Lys2190 or Lys2887 by converting those residues to tryptophan or tyrosine potentiated $Ca^{2+}$-dependent binding of [$^3$H]ryanodine to RyR2s (Fig. 4, ii and iii). These increases in $Ca^{2+}$-dependent binding of [$^3$H]ryanodine were not attributable to alterations in the amount of RyR2 protein used for assays (Fig. 4, insets). R1611G/K2190Y, R1611W/K2190Y, and K2190Y/K2887Y double-mutants exhibited reduced ability to bind [$^3$H]ryanodine (Fig. 4iv). Neutralizing the basic charge or neutralizing the charge and increasing the bulk at residues Arg4462 and Arg4682 (the mouse equivalent of Arg4683) reduced binding of [$^3$H]ryanodine (Fig. 4, v and vi).

**Planar Lipid Bilayer Assays.** To gain mechanistic insights regarding altered [$^3$H]ryanodine binding, wild-type and mutated RyR2s were purified and reconstituted into lipid bilayers and their gating and conductance were assayed as a function of cis (cytoplasmic) $Ca^{2+}$ levels. Figure 5i shows representative 1-s recordings of the cis $Ca^{2+}$ responsiveness of wild-type, single-mutant (K2190Y, K2887W, R4462W, and R4682G), and double-mutant (R1611G/K2190Y, R1611W/K2190Y, and K2190Y/K2887Y) receptors at +35 mV, in symmetric 250 mM KCl. Arg1611 mutants were not assayed because they did not show alterations in $Ca^{2+}$-dependent [$^3$H]ryanodine binding. K2190Y and K2887W, which showed enhanced $Ca^{2+}$-dependent [$^3$H]ryanodine binding, were more responsive to low cis $Ca^{2+}$ levels (0.1–1 $\mu$M), as indicated by their increased open probabilities (Fig. 5i). The responsiveness of K2190Y was similar to that of wild-type RyR2 at higher $Ca^{2+}$ levels, but K2887W was inactivated at lower $Ca^{2+}$ levels (deactivation $EC_{50}$ = 20 $\mu$M, compared with 3 mM for wild-type RyR2) (Fig. 5ii). R1611G/K2190Y, R1611W/K2190Y, and K2190Y/K2887Y double-mutants showed reduced responsiveness to low and high cis $Ca^{2+}$ levels. R4462W and R4682G mutants also exhibited reduced responsiveness to cis $Ca^{2+}$ levels, with channels, attaining maximal open probability values of 0.42 and 0.37 with 1000 and 100 $\mu$M $Ca^{2+}$, respectively (Fig. 5, i and ii).

In addition to alterations in cis $Ca^{2+}$ responsiveness, the conductances of K2190Y, K2887W, R4462G, R4682W, R1611G/K2190Y, and R1611W/K2190Y channels were ~10% lower than that of wild-type RyR2 ($p < 0.05$) (Fig. 5iii). The conductance of the double-mutant K2190Y/K2887Y was similar to that of wild-type RyR2 (Fig. 5iii).

**Transfection of RyR2s into HEK-293T Cells and Responsiveness of Cells to Extracellular $Ca^{2+}$.** We next set out to determine whether mutant channels exhibited altered $Ca^{2+}$ responsiveness inside cells. Less than 3% of the ≥150 HEK-293T cells transfected with wild-type RyR2 showed intracellular $Ca^{2+}$ oscillations in medium containing 0.2 or 0.4 mM $Ca^{2+}$ (Fig. 6). Increases in the $Ca^{2+}$ concentration in the medium to 1.0 or 1.8 mM only modestly increased intracellular $Ca^{2+}$ oscillations in cells transfected with wild-type RyR2 [8 (5%) of 150 cells]. Less than 3% of cells (4 of 149 cells) transfected with R4462Y, a mutant with reduced cis $Ca^{2+}$ responsiveness, exhibited intracellular $Ca^{2+}$ oscillations in medium with $Ca^{2+}$ concentrations ranging from 0.2 to 1.8 mM (Fig. 6). However, cells transfected with K2887W, a mutant with enhanced $Ca^{2+}$ responsiveness, exhibited enhanced $Ca^{2+}$ oscillations in media with low and high $Ca^{2+}$ concentrations [0.2 mM $Ca^{2+}$, 9 (6%) of 154 cells; 0.6 mM $Ca^{2+}$, 25 (16%) of 154 cells; 1.8 mM $Ca^{2+}$, 35 (23%) of 154 cells]. All cells assayed generated $Ca^{2+}$ transients when challenged with 10 mM caffeine, which indicated that the cells contained functional RyR2s. These data strongly suggested that carbonylation could induce aberrant opening and/or closing of RyR2s inside myocytes.

### RCS Modulation of RyR2s and Triggering of $Ca^{2+}$ Release from SR

We proceeded to determine whether RCS could alter the activity of RyR2s in vitro and in vivo. The prototype RCS chosen for this study was MGO.

**Effects of MGO on Binding of [$^3$H]Ryanodine to RyR2s.** In competition [$^3$H]ryanodine binding assays conducted with a free cytoplasmic $Ca^{2+}$ concentration of 300 $\mu$M, MGO initially enhanced binding and then displaced ryanodine from RyR2s in two phases. The $K_{i1}$ for phase A displacement was 25.0 ± 2.5 $\mu$M, and the $K_{i2}$ for phase B displacement was 400.5 ± 10.2 $\mu$M (Fig. 7i). The displacement curve for MGO was not parallel to that for ryanodine (data not shown), which suggests that MGO and ryanodine interact at different sites on RyR2. In a more-extensive study, we found that pretreating membrane vesicles with 15 $\mu$M MGO for 30 min increased the amount of [$^3$H]ryanodine bound to RyR2s at all $Ca^{2+}$ concentrations tested (Fig. 7ii). Pretreatment with 200 or 400 $\mu$M MGO enhanced binding of [$^3$H]ryanodine to RyR2s at lower $Ca^{2+}$ concentrations (0.1–13 $\mu$M) but reduced [$^3$H]ryanodine binding at higher $Ca^{2+}$ concentrations (70–3900 $\mu$M) (Fig. 7ii).

**Lipid Bilayer Assays.** To gain mechanistic insights, purified RyR2s were reconstituted into lipid bilayers and the effects of MGO on gating and conductance were determined.

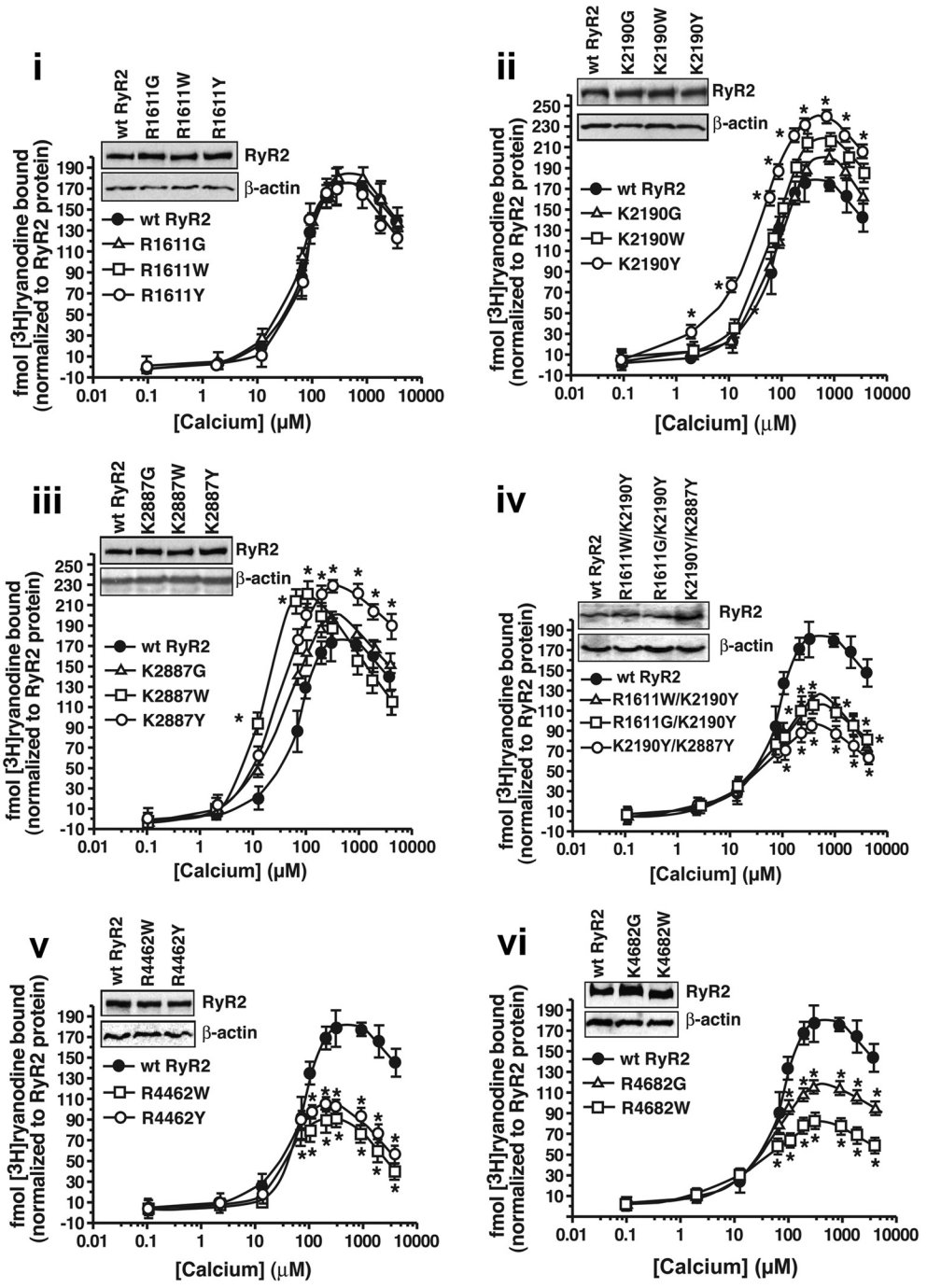


**Fig. 4.** Alterations in $Ca^{2+}$-dependent binding of [$^3$H]ryanodine to RyR2s with mutations to mimic carbonylation. Insets, equal amounts of RyR2 protein were used for this study. i, wild-type (wt) and Arg1611 mutant RyR2s. ii, wild-type and Lys2190 mutant RyR2s. iii, wild-type and Lys2887 mutant RyR2s. iv, wild-typeand Arg1611, Lys2190, and Lys2887 double-mutant RyR2s. v, wild-type and Arg4462 mutant RyR2s; vi, wild-type and Arg4682 mutant RyR2s. Data represent mean ± S.E.M. values from four experiments. *, significantly different from wild-type RyR2s ($p < 0.05$).

Addition of 16 $\mu$M MGO to the cis chamber of the lipid bilayer chamber (cis $Ca^{2+}$ concentration of 3.3 $\mu$M and symmetric KCl concentrations of 250 mM, +35 mV) increased the RyR2 open probability (from 0.21 to 0.51; $p < 0.05$) within 1 min after addition (Fig. 7, iii and iv). The increase in open probability was seen at both positive and negative holding potentials and resulted predominantly from an increase in the open state dwell time (from 1.5 to 5.7 ms; $p < 0.05$). Increasing the MGO concentration in the cis chamber further (32–80 $\mu$M) dose-dependently reduced the RyR2 open probability from 0.51 to 0.05 (Fig. 7, iii and iv). MGO concentrations of >40 $\mu$M significantly ($p < 0.05$) reduced RyR2 conductance (Fig. 7, iii and v).

**MGO Effects on $Ca^{2+}$ Release from SR.** [$^3$H]Ryanodine binding and lipid bilayer assays indicated that MGO altered the responsiveness of RyR2s to cytoplasmic $Ca^{2+}$. We sought to determine whether MGO could alter the activity of RyR2s inside cardiac myocytes. Time-lapse images for 1 of 24 quiescent myocytes exposed to MGO are shown in Fig. 8i. Ten seconds after the addition of MGO (25 $\mu$M), spontaneous $Ca^{2+}$ release increased at random locations within the myocyte. This increase in spontaneous $Ca^{2+}$ release persisted for 37 to 45 s, depending on the cell, and then transitioned into a $Ca^{2+}$ wave that lasted ~2.5 s and triggered myocyte contraction. Nuclear $Ca^{2+}$ levels also increased after the $Ca^{2+}$ wave. Removal of $Ca^{2+}$ from the medium did not alter the

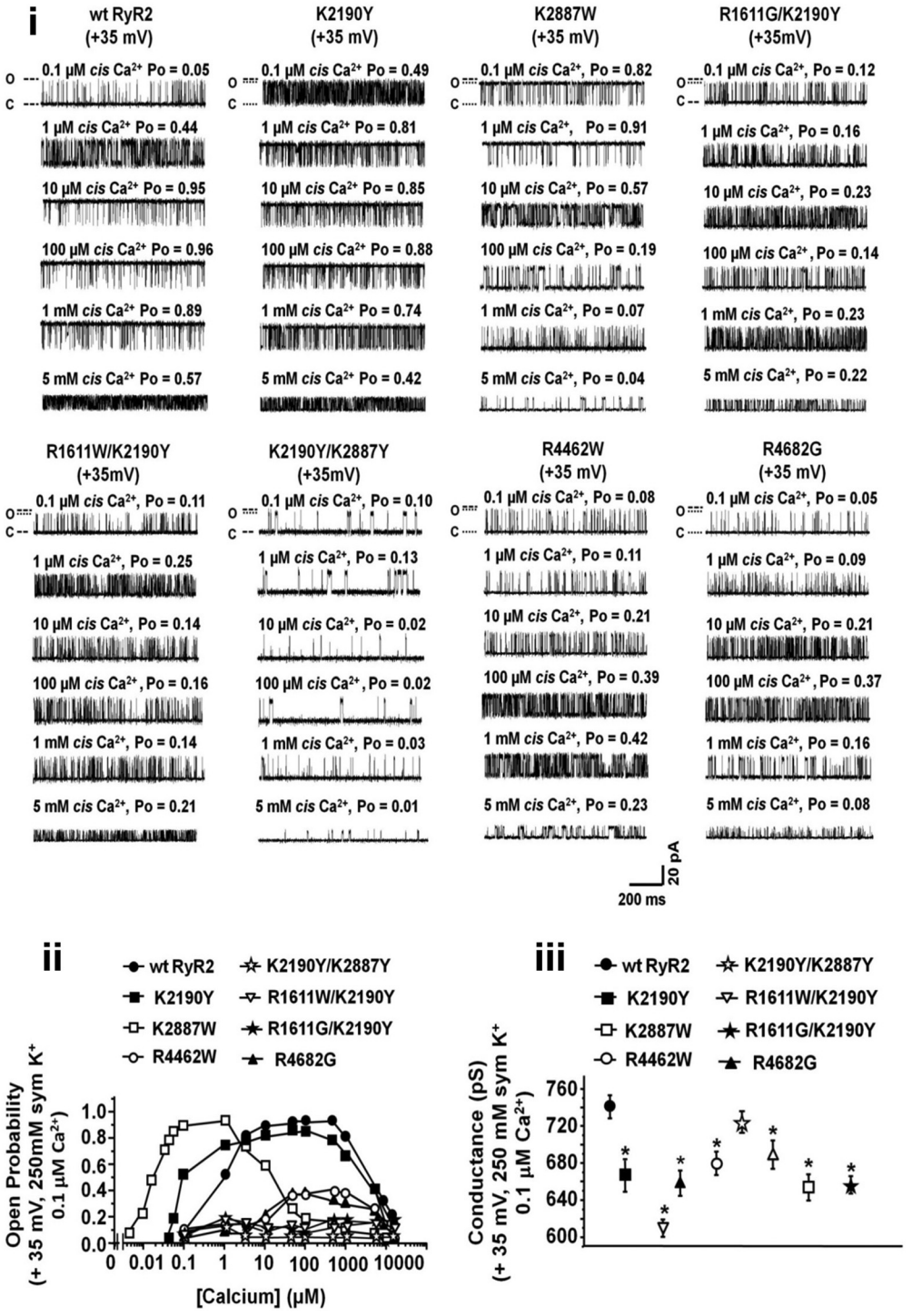


**Fig. 5.** Alterations in cytoplasmic $Ca^{2+}$ responsiveness of RyR2s with mutations to mimic carbonylation. i, representative, 1-s, single-channel responses of wild-type (wt) and mutated RyR2s to increasing cis $Ca^{2+}$ levels. Po, open probability; o, open; c, closed. ii, mean open probability values for at least nine channels for each mutant. S.E.M. values were between 4 and 8% and were omitted for clarity. iii, mean conductance values for wild-type and mutated RyR2s. *, significantly different from wild-type RyR2s ($p < 0.05$).

ability of MGO to alter spontaneous $Ca^{2+}$ release and generation of $Ca^{2+}$ waves (data not shown), which indicated that MGO was triggering $Ca^{2+}$ release from the SR.

Line-scan studies were conducted with 0.25-Hz field stimulation. Within 15 s after the addition of MGO (20 $\mu$M), spontaneous $Ca^{2+}$ release from the SR increased 12.8-fold in 18 of 22 of myocytes ($Ca^{2+}$ spark frequency before the addition of MGO was 1.8 $\pm$ 0.5 sparks/s in 50 $\mu$m, compared with 21.6 $\pm$ 1.2 sparks/s in 50 $\mu$m after MGO addition; $p < 0.05$) (Fig. 8ii). The increase in $Ca^{2+}$ spark frequency continued for 30 $\pm$ 6 s. In 66% of myocytes (12 of 18 cells), $Ca^{2+}$ sparks transitioned into $Ca^{2+}$ waves (Fig. 8ii). These $Ca^{2+}$ waves reduced the amplitude of evoked $Ca^{2+}$ transients (from 4.8 $\pm$ 0.4 fluorescence absorbance units after MGO addition but before the wave to 4.0 $\pm$ 0.2 fluorescence absorbance units after MGO addition and after the wave). Evoked $Ca^{2+}$ release from the SR after MGO treatment was dyssynchronous, akin to that seen in diabetic myocytes (Fig. 7ii). Spontaneous and evoked $Ca^{2+}$ cycling ceased in 18 (80%) of 22 cells, 5 min after the addition of MGO. The addition of caffeine (10 mM) to myocytes after cessation of evoked $Ca^{2+}$ transients triggered $Ca^{2+}$ release from the SR, but the amplitude was

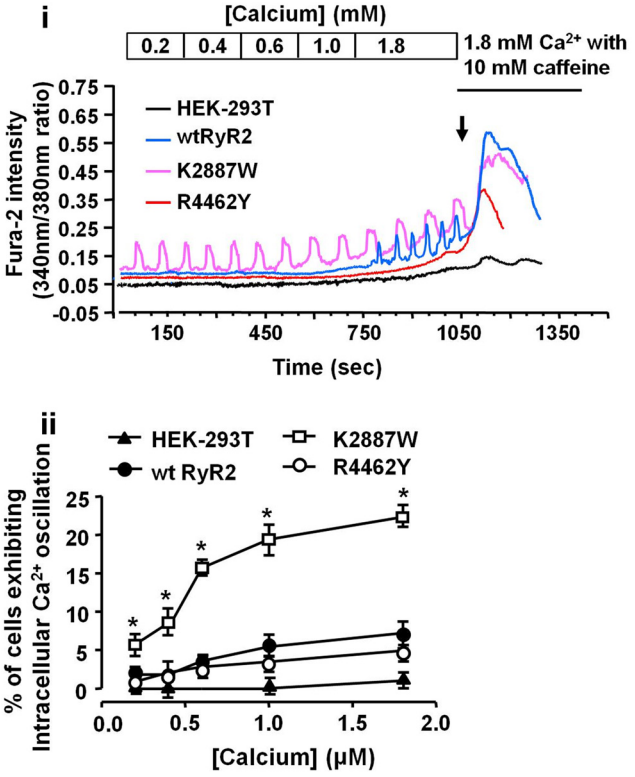


**Fig. 6.** Altered cellular $Ca^{2+}$ responsiveness of RyR2s with carbonylation-mimicking mutations. i, representative intracellular $Ca^{2+}$-cycling traces of HEK-293T cells transfected with K2888W, R4462Y, or wild-type (wt) RyR2 and subjected to increasing concentrations of $Ca^{2+}$ in the medium. Black arrow, start of caffeine challenge, which continued for 300 s. ii, mean number of cells exhibiting intracellular $Ca^{2+}$ oscillations as a function of the $Ca^{2+}$ concentration in the medium (five experiments with >30 cells for each mutant). *, significantly different from wild-type RyR2s ($p < 0.05$).

significantly reduced (31.9 ± 7.7% of that generated in untreated myocytes; eight cells).

### Effects of MGO on Mitochondrial Production of Superoxide/ROS

Previous studies showed that MGO increased mitochondrial superoxide/ROS production (Du et al., 2001). Time-lapsed confocal microscopy was used to ascertain whether changes in intracellular $Ca^{2+}$ homeostasis induced by MGO resulted from MGO acting directly on RyR2s or from the superoxide/ROS produced acting on RyR2s. Addition of MGO (20 μM) to freshly isolated rat ventricular myocytes (16 cells) increased mitochondrial superoxide and total ROS production. However, this increase started ~8 to 9 min after the addition of MGO (Fig. 9, i and iv). Analyses of Z-stack images of mitochondria (MitoTracker Green), mitochondrial superoxide (405-nm excitation of MitoSOX), and mitochondrial total ROS (488-nm excitation of MitoSOX) before and after MGO addition revealed a 210.5 ± 6.4% increase in superoxide levels 15 min after MGO addition (seven cells) (Fig. 9, ii and iii) and a 758.9 ± 12.2% increase in total ROS levels 16 min after MGO addition (seven cells) (Fig. 9, v and vi). Increasing MGO to 40 μM decreased the time to detection of mitochondrial superoxide and total ROS production to ~3 min and increased the amount of superoxide and total ROS produced (data not shown).

### Blunting of RyR2 Dysregulation through Treatment with RCS Scavengers

We reported previously that treatment of diabetic rats with the RCS scavengers Ag and Py blunted reductions in cardiac and myocyte function (Shao et al., 2010, 2011). These drugs did not alter serum glucose levels but decreased serum semicarbazide-sensitive amine oxidase activity and levels of thiobarbituric acid-reactive substances (principally malondialdehyde) (Table 1). In this study, treatment of diabetic rats with Py and Ag blunted the increase in $Ca^{2+}$ spark frequency (Fig. 10i). Py and Ag treatments prevented the formation of carbonyl adducts on RyR2s (Fig. 10, ii and iii). Py treatment reduced $N^{\epsilon}$-carboxy(methyl)lysine adduct levels by 79.2 ± 5.1%, pentosidine adduct levels by 86.4 ± 8.2%, pyrraline adduct levels by 88.3 ± 12.1%, and 3-deoxyglucosone/hydroimidazole levels by 89.1 ± 11.2%. Ag treatment was less effective, reducing $N^{\epsilon}$-carboxy(methyl)lysine adduct levels by 48.1 ± 7.2%, pentosidine adduct levels by 38.1 ± 9.1%, pyrraline adduct levels by 67.1 ± 9.1%, and 3-deoxyglucosone/hydroimidazole levels by 58 ± 13% (Fig. 10iii). Py and Ag treatments did not alter the expression of RyR2s in diabetes but enhanced their ability to bind [$^3$H]ryanodine (Fig. 10iv). The amplitude of caffeine-induced $Ca^{2+}$ transients in diabetic myocytes was 52% less than that in control myocytes (0.37 ± 0.02 versus 0.76 ± 0.03 fluorescence absorbance units). Py and Ag treatments blunted the reduction in caffeine-induced $Ca^{2+}$ transient amplitudes to 80.2 ± 3.4 and 74.5 ± 4.5% of control values, respectively (Fig. 10v).

## Discussion

The principal finding of the present study is that the heterogeneity in RyR2 function seen in hearts of rats with STZ-induced diabetes stems in part from post-translational modification by RCS. These modifications alter the sensitivity of RyR2s to cytoplasmic $Ca^{2+}$, with some modifications enhancing cytoplasmic $Ca^{2+}$ responsiveness and others reducing the responsiveness of the channel to cytoplasmic $Ca^{2+}$. In this study, carbonyl adducts at five amino acid residues of RyR2s were confirmed. These residues by no means represent the complete list of amino acids of RyR2s that undergo carbonylation in diabetes. Elevated levels of pentosidine, $N^{\epsilon}$-carboxy(methyl)lysine, and GA-pyridine adducts on dRyR2s were detected through Western blotting, but their locations on RyR2s were not determined. Several reasons for the latter are likely, including reduced ionization efficiency of the carbonylated peptides, the inability of our Perl algorithm to locate cross-linking pentosidine adducts efficiently, and formation of some adducts at relatively low levels (Ahmed et al., 2003). Another reason might involve the method itself. In the present study, trypsin was used for digestion of RyR2s. This enzyme cleaves proteins at lysines and arginines; if a modification is present on either residue, then trypsin will not digest the protein. If GluC, which cleaves proteins at glutamyl residues, had been used for digestion of RyR2s, then more peptides with carbonyl adducts might have been obtained (Priego Capote and Sanchez, 2009).

A surprising finding of the present study is that RCS did not react indiscriminately with all available basic amino acid residues on RyR2s. Some residues (such as the ones identified) were more susceptible to carbonylation than others. One explanation for this finding might be the electronic environ-

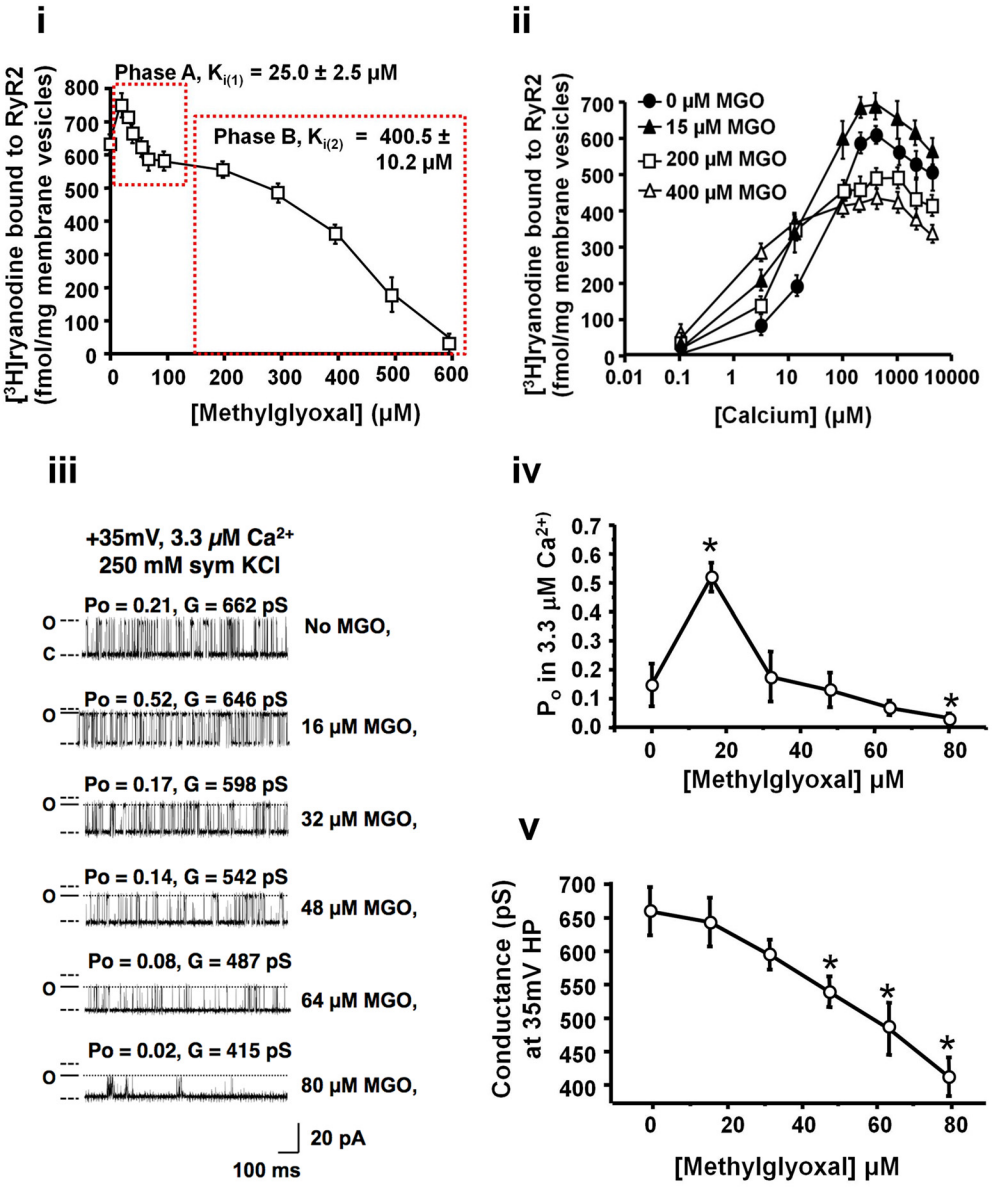


**Fig. 7.** Alteration of RyR2 activity by MGO. i, ability of MGO to displace [$^3$H]ryanodine from RyR2s. Data shown are the average of six experiments conducted with three separate membrane preparations. ii, effects of preincubation of SR membrane vesicles with varying amounts of MGO on $Ca^{2+}$-dependent binding of [$^3$H]ryanodine to RyR2s. Data shown are the average of six experiments performed with three separate membrane preparations. iii, representative, 1-s, single-channel responses of cRyR2s to increasing cis concentrations of MGO at a holding potential of +35 mV. sym, symmetric; o, open; c, closed. iv, open probability ($P_o$) (mean ± S.E.M.) values for cRyR2s with increasing MGO concentrations at a holding potential of +35 mV, with cis $Ca^{2+}$ levels of 3.3 μM and symmetric KCl concentrations of 250 mM (at least 10 channels). v, conductance (mean ± S.E.M.) values for RyR2s in response to increasing MGO concentrations at a holding potential (HP) of +35 mV, with cis $Ca^{2+}$ levels of 3.3 μM and symmetric KCl concentrations of 250 mM (at least 10 channels). *, significantly different from wild-type RyR2s ($p < 0.05$).

ment of these residues. Basic residues with low p$K_a$ values are more likely to undergo carbonylation than are residues with higher p$K_a$ values, because a greater fraction of low-p$K_a$ residues would exist in the deprotonated state at a physiological pH of 7.4, which would render them susceptible to modification (Iberg and Flückiger, 1986).

The present study indicates that the site and extent of modification dictate the effects of carbonylation on RyR2 function. In this study, mutation of Arg1611 had no significant impact on RyR2 function. This finding raises the possibility that some residues act as "sinks" to protect RyR2s from transient bursts in α-oxoaldehyde production that may occur. In contrast, mutations at Lys2190 or Lys2887 exaggerated the $Ca^{2+}$ responsiveness of RyR2. In the resting or nonactivated state, the N-terminal and central domains of RyR2 make close contacts in several regions, to maintain RyR2 in a closed state. Two such subdomains reside between amino acids 2000 and 2500 (Ikemoto and Yamamoto, 2002) and amino acids 2234 and 2750 (Suetomi et al., 2011). Because Lys2190 and Lys2887 reside on both sides of these domains, we speculate that these residues may be involved in "domain zipping" and modifying them may destabilize N-terminal domain-C-terminal domain interactions, leading to enhanced $Ca^{2+}$ responsiveness of RyR2.

Mutagenesis studies suggest that carbonylation at Arg4462 or Arg4682 likely would reduce the $Ca^{2+}$ responsiveness of RyR2. These residues reside within and immediately downstream of divergent region 1 (amino acids 4254–4631), which dictates the $Ca^{2+}$ sensitivity of ryanodine receptors (Du et al., 2000), and increasing bulk at these residues might compromise the ability of $Ca^{2+}$ to activate RyR2.

Our data showed that mutations at more than one site (Arg1611, Lys2190, and Lys2887) reduced the $Ca^{2+}$ responsiveness of RyR2 (Fig. 4), which suggests that, the more extensive the carbonylation is, the more likely it is that RyR2 activity would be reduced. More-extensive carbonylation could occur through greater duration of diabetes and/or higher glucose levels (more glucose-derived RCS generated). Because blood glucose levels in 15-week *db/db* mice are >30 mM, increased carbonylation of RyR2s may be a contributing

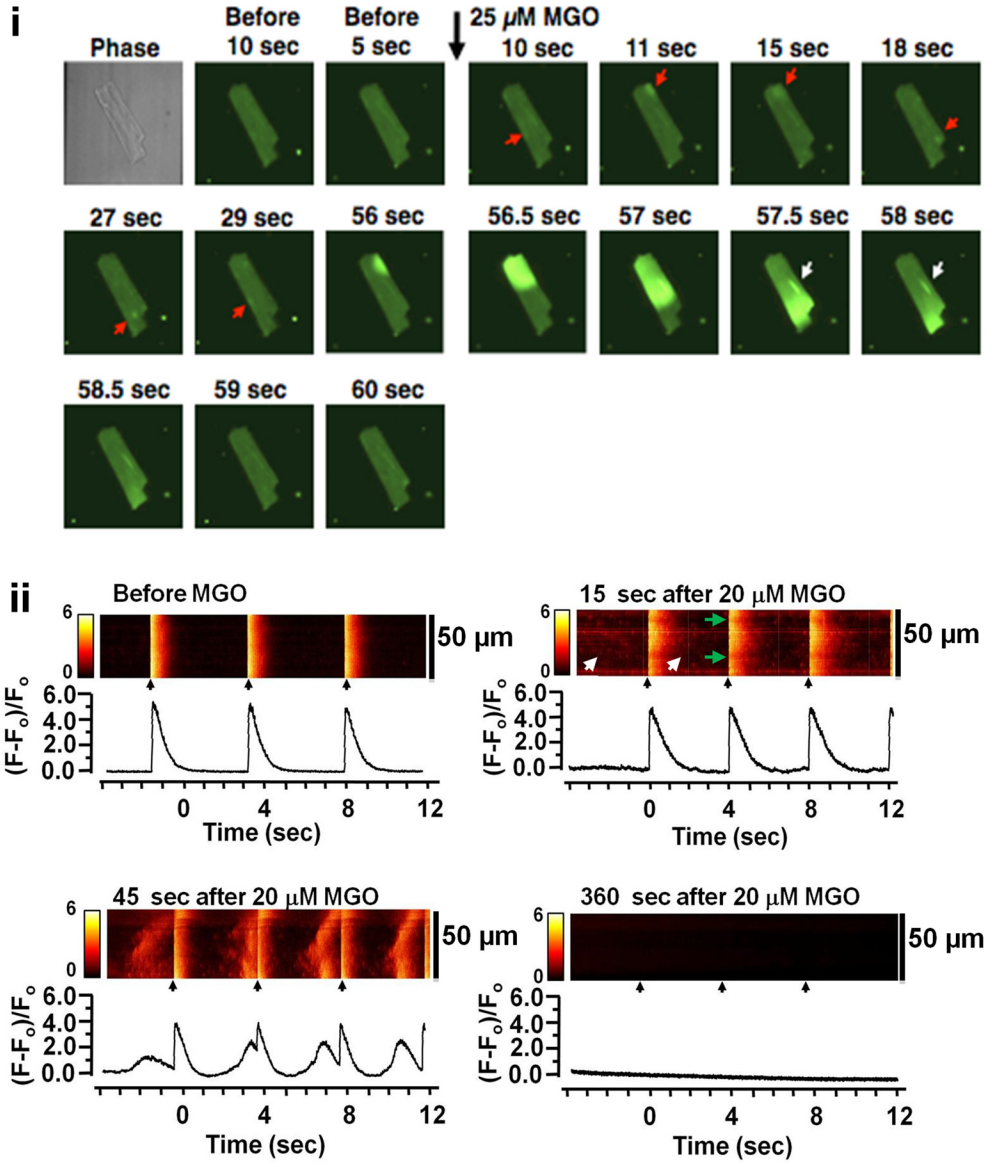


**Fig. 8.** Alteration of intracellular $Ca^{2+}$ homeostasis in healthy myocytes by MGO. i, time-lapse confocal images showing changes in intracellular $Ca^{2+}$ release in a myocyte acutely exposed to 20 $\mu$M MGO and monitored for >6 min. Red arrows, spontaneous $Ca^{2+}$ release. White arrows, elevations in nuclear $Ca^{2+}$ levels. Experiments were conducted with 18 cells from four separate myocyte preparations, all of which exhibited similar behavior when challenged with MGO. ii, representative line-scanned images of spontaneous and evoked $Ca^{2+}$ release in myocytes acutely exposed to 20 $\mu$M MGO and monitored for >6 min. Black arrows, stimulation at 0.25 Hz. White arrows, spontaneous $Ca^{2+}$ release. Green arrows, sites of nonuniform evoked $Ca^{2+}$ release. Experiments were conducted with 22 cells from four separate myocyte preparations, and 18 exhibited characteristics similar to those shown.

factor in the reduced frequency of $Ca^{2+}$ sparks reported for myocytes from these animals (Pereira et al., 2006). Factors other than high levels of glucose also may be involved in reducing the activity of RyR2 (Lacombe et al., 2007).

Through Western blotting, 2- to 5-fold increases in carbonyl adduct levels were found for dRyR2s. These are aggregate increases and do not indicate the extent to which individual RyR2 molecules are modified by RCS and how much of the total RyR2 protein amount in the cell undergoes carbonylation in diabetes. From [$^3$H]ryanodine binding studies, we know that ~30% of total dRyR2s exhibited reduced $Ca^{2+}$ responsiveness. The amount of RyR2 with enhanced $Ca^{2+}$ responsiveness is not known but we suspect that it may be significant, because the majority of channels assayed in an earlier study exhibited gain of function (Tian et al., 2011). It is important to note that more than one type of carbonyl adduct may be formed on a susceptible amino acid residue in diabetes. For example, both imidazolone A/B (derived from glyoxal/methylglyoxal) and argpyrimidine (derived from MGO) were found on Arg4462 of RyR2 in this study. Which type of adduct is formed on any particular residue may be dictated by the concentration of RCS present.

It has been known for more than 20 years that RCS and RCS adduct levels are elevated in the serum of individuals with diabetes (Makita et al., 1992; Slatter et al., 2004; Lapolla et al., 2005; Fosmark et al., 2009; Vicentini et al., 2011) and scavengers of RCS can prevent diabetic complications (Brownlee et al., 1986). Although RCS adduct-breaking strategies have been not been successful in clinical studies (Hartog et al., 2011), therapies involving agents that scavenge RCS and/or prevent RCS production have been successful (Bolton et al., 2004; Williams et al., 2007). Such drugs likely exert their beneficial effects through multiple mechanisms, including chelating metals involved in the synthesis of RCS (Nagai et al., 2012). In this study, we found that Py was more effective than Ag in reducing the carbonylation of RyR2 and normalizing its $Ca^{2+}$ responsiveness (activity). Might Py be more efficacious than Ag because its lower primary amine content allows it to enter myocytes? If this is the case, then cellular

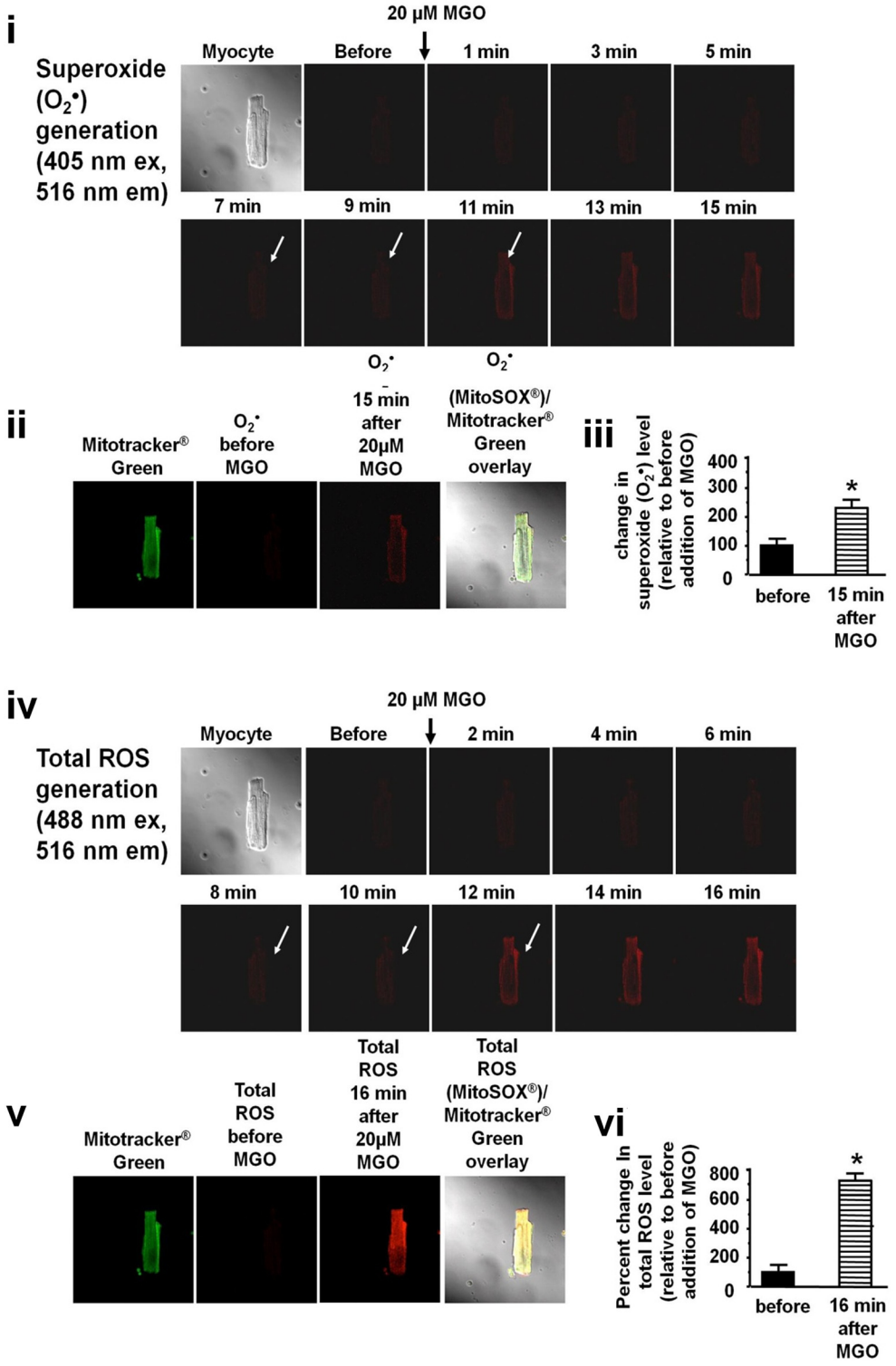


**Fig. 9.** Increased mitochondrial superoxide production with MGO. i and iv, time-lapse confocal images showing production of superoxide (i) and total ROS (iv) in a myocyte after exposure to 20 $\mu$M MGO. ex, excitation; em, emission. ii and v, mitochondrial localization and superoxide levels with MGO exposure. Green images, MitoTracker Green (mitochondria); red images, MitoSox signals monitored with 404-nm (ii) or 488-nm (v) excitation; right panels, green-red overlay images, showing superoxide and ROS in mitochondria. iii and vi, graphs showing production (mean ± S.E.M.) of superoxide (iii) and ROS (vi) in mitochondria before and 15 and 16 min, respectively, after MGO addition. *, significantly different from values before MGO addition ($p < 0.05$). White arrows indicate formation of superoxide and total ROS.

permeability may be an important consideration in the design of RCS-reducing therapies. It should be noted that we found in a previous study that glucose-derived MGO, the enzyme that synthesizes it (vascular adhesion protein-1/serum semicarbazide amine oxidase), and the enzyme that breaks it down (glyoxalase-1) were up-regulated in ventricular myocytes in diabetes (Shao et al., 2011). It is noteworthy that the MGO-derived argpyrimidine adduct was elevated on SERCA2 (Shao et al., 2011) and on RyR2 (Fig. 3ii).

The present study has limitations. First, none of the mutants created is ideal for mimicking the simultaneous charge neutralization and increase in bulk induced by carbonylation. Tryptophan has a hydrophobic side chain that might compromise protein folding, and tyrosine is a phosphorylatable residue that might alter RyR2 activity. Although alanine (and perhaps isoleucine/leucine) would have been a more-appropriate choice than glycine to mimic charge neutralization, we were fortunate that the characteristics of our glycine mutants paralleled those of the corresponding tyrosine and tryptophan mutants.

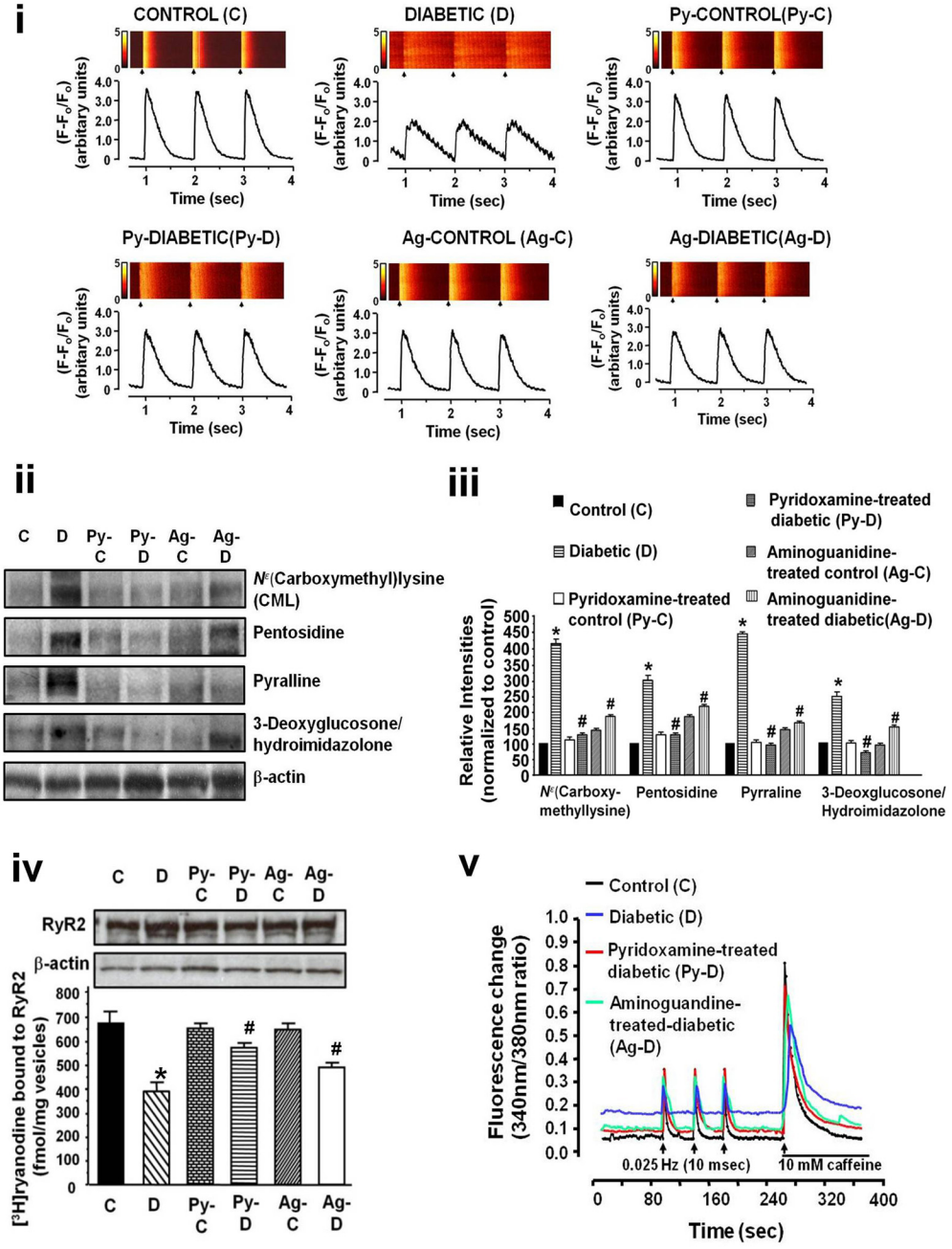


**Fig. 10.** Treatment of diabetic rats with scavengers of reactive carbonyl species, blunting RyR2 dysregulation. i, representative evoked $Ca^{2+}$ transients in ventricular myocytes isolated from control, diabetic, Py-treated control, Py-treated diabetic, Ag-treated control, and Ag-treated diabetic rats. Myocytes were stimulated at 1 Hz (black arrow). Experiments were conducted with ≥30 cells from four separate myocyte preparations per experimental group. ii, representative autoradiograms of carbonyl adducts in ventricular heart homogenates from diabetic, Py-treated control, Py-treated diabetic, Ag-treated control, and Ag-treated diabetic rats. Experiments were conducted with four separate junctional SR vesicle preparations. iii, relative intensity values (mean ± S.E.M.). ∗, significantly different from control value ($p < 0.05$); #, significantly different from diabetic value ($p < 0.05$). iv, representative autoradiograms indicating steady-state levels of RyR2 and β-actin proteins in membrane vesicles isolated from hearts of control, diabetic, Py-treated control, Py-treated diabetic, Ag-treated control, and Ag-treated diabetic rats. Graph, ability of equivalent amounts of RyR2 protein from control, diabetic, Py-treated control, Py-treated diabetic, Ag-treated control, and AG-treated diabetic hearts to bind [$^3$H]ryanodine. Experiments were conducted at least five times, with four different membrane preparations. ∗, significantly different from control value ($p < 0.05$); #, significantly different from diabetic value ($p < 0.05$). v, representative caffeine-induced $Ca^{2+}$ transients in ventricular myocytes isolated from control, diabetic, Py-treated control, Py-treated diabetic, Ag-treated control, and Ag-treated diabetic hearts. First three black arrows, electrically evoked stimulation; last black arrow, application of caffeine. Experiments were performed five times.

Second, we and others showed that SERCA2 activity in the myocardium was reduced in diabetes (Belke et al., 2004; Shao et al., 2011). In addition to affecting the rate and amount of $Ca^{2+}$ transport from the cytoplasm to the lumen of the SR (i.e., SR $Ca^{2+}$ content), reductions in SERCA2 levels would elevate diastolic $Ca^{2+}$ levels, which could increase the activity of RyR2. In a recent study, we found that SERCA2 was extensively modified by RCS in diabetes and that treatment of diabetic rats with Py prevented the carbonylation of SERCA2 and enhanced its activity (Shao et al., 2011). Therefore, the increase in $Ca^{2+}$ sparks seen in diabetic myocytes and the reduction in $Ca^{2+}$ sparks seen in myocytes from Py- and Ag-treated rats may be attributable in part to alterations in SERCA2 activity.

Third, in addition to regulation by cytoplasmic $Ca^{2+}$, the activity of RyR2 is regulated by an array of other cytoplasmic ligands and proteins and by luminal $Ca^{2+}$. Whether the carbonylation-mimicking RyR2 mutations altered the responsiveness of RyR2 to activating/deactivating ligands such as ATP, cADP-ribose, and $Mg^{2+}$ and whether the mutants would exhibit altered luminal $Ca^{2+}$ responsiveness remain to be determined. It is not clear whether RCS adducts alter the binding of proteins, including FK506 binding protein 12.6, protein phosphatase 2, and calmodulin, to RyR2.

Fourth, it is unlikely that MGO increases $Ca^{2+}$ sparks in myocytes solely through its action on RyR2. MGO also acts on SERCA2, which can affect RyR2 activity. It is possible that MGO also alters the redox status of mitochondria, which would directly affect the activity of RyR2 (Zhou et al., 2011). On the basis of the findings of the present study, however, MGO's actions on mitochondria occur after those on SR $Ca^{2+}$-cycling proteins. MGO was used as a prototype RCS, and its

effects on intracellular $Ca^{2+}$ homeostasis and RyR2 function occurred very quickly (seconds to minutes). Although this rapid modification with MGO emphasizes our point that RyR2 is a molecular target, we do not have any data on the kinetics of action of other RCS, such as malondialdehyde, 4-hydroxynonenal, and glucosone.

In conclusion, this study identifies carbonylation as a novel mechanism that contributes to RyR2 dysregulation (functional heterogeneity) in diabetes. Limited carbonylation enhances or reduces the cytoplasmic $Ca^{2+}$ responsiveness of RyR2 (depending on the site of carbonylation), whereas extensive carbonylation reduces the cytoplasmic $Ca^{2+}$ responsiveness of RyR2. Aberrant opening of RyR2 resulting from enhanced $Ca^{2+}$ responsiveness would induce delayed afterdepolarization and arrhythmias (Lehnart et al., 1998; Marks, 2002; Watanabe and Knollmann, 2011), whereas decreased $Ca^{2+}$ responsiveness of RyR2 would reduce the amplitude of evoked $Ca^{2+}$ release from the SR and muscle contraction, phenotypes that are commonly seen among individuals with diabetes mellitus. Reductions in RCS levels blunted RyR2 dysregulation in diabetes. These new data suggest that myocyte-permeant RCS scavengers may be useful as an adjunct therapy to slow the development of heart failure in individuals with diabetes.

#### Acknowledgments

We thank Dr. Clara Franzini-Armstrong (University of Pennsylvania) for assistance with electron-microscopic studies of dyad junctions, Dr. Wayne Chen (University of Calgary) for provision of mouse cDNA encoding RyR2, Dr. Gerhard Meissner (University of North Carolina) for assistance with bilayer preparation, and Dr. Mu Wang (Indiana University School of Medicine) for assistance with early mass spectrometric analyses. We also thank Janice A. Taylor and James R. Talaska (Confocal Laser Scanning Microscope Core Facility, University of Nebraska Medical Center) for assistance with confocal microscopy.

#### Authorship Contributions

*Participated in research design:* Rozanski, Singh, and Bidasee.

*Conducted experiments:* Shao, Tian, Ouyang, Moore, Alomar, D'Souza, and Bidasee.

*Contributed new reagents or analytic tools:* Nemet and Nagai.

*Performed data analysis:* Shao, Tian, Ouyang, Moore, Alomar, Kutty, Ramanadham, and Bidasee.

*Wrote or contributed to the writing of the manuscript:* Moore, Kutty, Rozanski, Ramanadham, Singh, and Bidasee.

#### References

Ahmed N, Thornalley PJ, Dawczynski J, Franke S, Strobel J, Stein G, and Haik GM (2003) Methylglyoxal-derived hydroimidazolone advanced glycation end-products of human lens proteins. *Invest Ophthalmol Vis Sci* **44:**5287–5292.

Barrera G, Pizzimenti S, and Dianzani MU (2004) 4-Hydroxynonenal and regulation of cell cycle: effects on the pRb/E2F pathway. *Free Radic Biol Med* **37:**597–606.

Baynes JW and Thorpe SR (1999) Role of oxidative stress in diabetic complications: a new perspective on an old paradigm. *Diabetes* **48:**1–9.

Belke DD, Swanson EA, and Dillmann WH (2004) Decreased sarcoplasmic reticulum activity and contractility in diabetic *db/db* mouse heart. *Diabetes* **53:**3201–3208.

Bertoni AG, Hundley WG, Massing MW, Bonds DE, Burke GL, and Goff DC Jr (2004) Heart failure prevalence, incidence, and mortality in the elderly with diabetes. *Diabetes Care* **27:**699–703.

Bidasee KR, Dinçer UD, and Besch HR Jr (2001) Ryanodine receptor dysfunction in hearts of streptozotocin-induced diabetic rats. *Mol Pharmacol* **60:**1356–1364.

Bidasee KR, Nallani K, Yu Y, Cocklin RR, Zhang Y, Wang M, Dincer UD, and Besch HR Jr (2003) Chronic diabetes increases advanced glycation end products on cardiac ryanodine receptors/calcium-release channels. *Diabetes* **52:**1825–1836.

Bolton WK, Cattran DC, Williams ME, Adler SG, Appel GB, Cartwright K, Foiles PG, Freedman BI, Raskin P, Ratner RE, et al. (2004) Randomized trial of an inhibitor of formation of advanced glycation end products in diabetic nephropathy. *Am J Nephrol* **24:**32–40.

Bracken N, Howarth FC, and Singh J (2006) Effects of streptozotocin-induced diabetes on contraction and calcium transport in rat ventricular cardiomyocytes. *Ann NY Acad Sci* **1084:**208–222.

Brownlee M, Vlassara H, Kooney A, Ulrich P, and Cerami A (1986) Aminoguanidine prevents diabetes-induced arterial wall protein cross-linking. *Science* **232:**1629–1632.

Chen C and Okayama H (1987) High-efficiency transformation of mammalian cells by plasmid DNA. *Mol Cell Biol* **7:**2745–2752.

Choi KM, Zhong Y, Hoit BD, Grupp IL, Hahn H, Dilly KW, Guatimosim S, Lederer WJ, and Matlib MA (2002) Defective intracellular $Ca^{2+}$ signaling contributes to cardiomyopathy in type 1 diabetic rats. *Am J Physiol Heart Circ Physiol* **283:**H1398–H1408.

Dalle-Donne I, Aldini G, Carini M, Colombo R, Rossi R, and Milzani A (2006) Protein carbonylation, cellular dysfunction, and disease progression. *J Cell Mol Med* **10:**389–406.

Du GG, Khanna VK, and MacLennan DH (2000) Mutation of divergent region 1 alters caffeine and $Ca^{2+}$ sensitivity of the skeletal muscle $Ca^{2+}$ release channel (ryanodine receptor). *J Biol Chem* **275:**11778–11783.

Du J, Suzuki H, Nagase F, Akhand AA, Ma XY, Yokoyama T, Miyata T, and Nakashima I (2001) Superoxide-mediated early oxidation and activation of ASK1 are important for initiating methylglyoxal-induced apoptosis process. *Free Radic Biol Med* **31:**469–478.

Ellis EM (2007) Reactive carbonyls and oxidative stress: potential for therapeutic intervention. *Pharmacol Ther* **115:**13–24.

Ferrington DA, Krainev AG, and Bigelow DJ (1998) Altered turnover of calcium regulatory proteins of the sarcoplasmic reticulum in aged skeletal muscle. *J Biol Chem* **273:**5885–5891.

Fosmark DS, Berg JP, Jensen AB, Sandvik L, Agardh E, Agardh CD, and Hanssen KF (2009) Increased retinopathy occurrence in type 1 diabetes patients with increased serum levels of the advanced glycation endproduct hydroimidazolone. *Acta Ophthalmol* **87:**498–500.

Hartog JW, Willemsen S, van Veldhuisen DJ, Posma JL, van Wijk LM, Hummel YM, Hillege HL, Voors AA, and BENEFICIAL investigators (2011) Effects of alagebrium, an advanced glycation endproduct breaker, on exercise tolerance and cardiac function in patients with chronic heart failure. *Eur J Heart Fail* **13:**899–908.

Iberg N and Flückiger R (1986) Nonenzymatic glycosylation of albumin in vivo. Identification of multiple glycosylated sites. *J Biol Chem* **261:**13542–13545.

Ikemoto N and Yamamoto T (2002) Regulation of calcium release by interdomain interaction within ryanodine receptors. *Front Biosci* **7:**d671–d683.

Jourdon P and Feuvray D (1993) Calcium and potassium currents in ventricular myocytes isolated from diabetic rats. *J Physiol* **470:**411–429.

Lacombe VA, Viatchenko-Karpinski S, Terentyev D, Sridhar A, Emani S, Bonagura JD, Feldman DS, Györke S, and Carnes CA (2007) Mechanisms of impaired calcium handling underlying subclinical diastolic dysfunction in diabetes. *Am J Physiol Regul Integr Comp Physiol* **293:**R1787–R1797.

Lapolla A, Flamini R, Lupo A, Aricò NC, Rugiu C, Reitano R, Tubaro M, Ragazzi E, Seraglia R, and Traldi P (2005) Evaluation of glyoxal and methylglyoxal levels in uremic patients under peritoneal dialysis. *Ann NY Acad Sci* **1043:**217–224.

Lehnart SE, Schillinger W, Pieske B, Prestle J, Just H, and Hasenfuss G (1998) Sarcoplasmic reticulum proteins in heart failure. *Ann NY Acad Sci* **853:**220–230.

Ligeti L, Szenczi O, Prestia CM, Szabó C, Horváth K, Marcsek ZL, van Stiphout RG, van Riel NA, Op den Buijs J, Van der Vusse GJ, et al. (2006) Altered calcium handling is an early sign of streptozotocin-induced diabetic cardiomyopathy. *Int J Mol Med* **17:**1035–1043.

Ling X, Sakashita N, Takeya M, Nagai R, Horiuchi S, and Takahashi K (1998) Immunohistochemical distribution and subcellular localization of three distinct specific molecular structures of advanced glycation end products in human tissues. *Lab Invest* **78:**1591–1606.

Luo D, Sun H, Xiao RP, and Han Q (2005) Caffeine induced $Ca^{2+}$ release and capacitative $Ca^{2+}$ entry in human embryonic kidney (HEK293) cells. *Eur J Pharmacol* **509:**109–115.

Makita Z, Vlassara H, Rayfield E, Cartwright K, Friedman E, Rodby R, Cerami A, and Bucala R (1992) Hemoglobin-AGE: a circulating marker of advanced glycosylation. *Science* **258:**651–653.

Marks AR (2002) Ryanodine receptors, FKBP12, and heart failure. *Front Biosci* **7:**d970–d977.

Mitra R and Morad M (1985) A uniform enzymatic method for dissociation of myocytes from hearts and stomachs of vertebrates. *Am J Physiol* **249:**H1056–H1060.

Nagai R, Fujiwara Y, Mera K, Motomura K, Iwao Y, Tsurushima K, Nagai M, Takeo K, Yoshitomi M, Otagiri M, et al. (2008) Usefulness of antibodies for evaluating the biological significance of AGEs. *Ann NY Acad Sci* **1126:**38–41.

Nagai R, Horiuchi S, and Unno Y (2003) Application of monoclonal antibody libraries for the measurement of glycation adducts. *Biochem Soc Trans* **31:**1438–1440.

Nagai R, Murray DB, Metz TO, and Baynes JW (2012) Chelation: a fundamental mechanism of action of AGE inhibitors, AGE breakers, and other inhibitors of diabetes complications. *Diabetes* **61:**549–559.

Nagaraj RH, Oya-Ito T, Padayatti PS, Kumar R, Mehta S, West K, Levison B, Sun J, Crabb JW, and Padival AK (2003) Enhancement of chaperone function of alpha-crystallin by methylglyoxal modification. *Biochemistry* **42:**10746–10755.

Institute of Laboratory Animal Resources (1996) *Guide for the Care and Use of Laboratory Animals* 7th ed. Institute of Laboratory Animal Resources, Commission on Life Sciences, National Research Council, Washington DC.

Nemet I, Varga-Defterdarović L, and Turk Z (2004) Preparation and quantification of methylglyoxal in human plasma using reverse-phase high-performance liquid chromatography. *Clin Biochem* **37:**875–881.

Netticadan T, Temsah RM, Kent A, Elimban V, and Dhalla NS (2001) Depressed levels of $Ca^{2+}$-cycling proteins may underlie sarcoplasmic reticulum dysfunction in the diabetic heart. *Diabetes* **50:**2133–2138.

Oya T, Hattori N, Mizuno Y, Miyata S, Maeda S, Osawa T, and Uchida K. (1999)

Methylglyoxal modification of protein. Chemical and immunochemical characterization of methylglyoxal-arginine adducts. *J Biol Chem* **274:**18492–184502.
Pereira L, Matthes J, Schuster I, Valdivia HH, Herzig S, Richard S, and Gómez AM (2006) Mechanisms of $[Ca^{2+}]_i$ transient decrease in cardiomyopathy of *db/db* type 2 diabetic mice. *Diabetes* **55:**608–615.
Priego Capote F and Sanchez JC (2009) Strategies for proteomic analysis of non-enzymatically glycated proteins. *Mass Spectrom Rev* **28:**135–146.
Segré CV and Chiocca S (2011) Regulating the regulators: the post-translational code of class I HDAC1 and HDAC2. *J Biomed Biotechnol* **2011:**690848–690863.
Shao CH, Capek HL, Patel KP, Wang M, Tang K, DeSouza C, Nagai R, Mayhan W, Periasamy M, and Bidasee KR (2011) Carbonylation contributes to SERCA2a activity loss and diastolic dysfunction in a rat model of type 1 diabetes. *Diabetes* **60:**947–959.
Shao CH, Rozanski GJ, Nagai R, Stockdale FE, Patel KP, Wang M, Singh J, Mayhan WG, and Bidasee KR (2010) Carbonylation of myosin heavy chains in rat heart during diabetes. *Biochem Pharmacol* **80:**205–217.
Shao CH, Rozanski GJ, Patel KP, and Bidasee KR (2007) Dyssynchronous (non-uniform) $Ca^{2+}$ release in myocytes from streptozotocin-induced diabetic rats. *J Mol Cell Cardiol* **42:**234–246.
Shao CH, Wehrens XH, Wyatt TA, Parbhu S, Rozanski GJ, Patel KP, and Bidasee KR (2009) Exercise training during diabetes attenuates cardiac ryanodine receptor dysregulation. *J Appl Physiol* **106:**1280–1292.
Slatter DA, Avery NC, and Bailey AJ (2004) Identification of a new cross-link and unique histidine adduct from bovine serum albumin incubated with malondialdehyde. *J Biol Chem* **279:**61–69.
Suetomi T, Yano M, Uchinoumi H, Fukuda M, Hino A, Ono M, Xu X, Tateishi H, Okuda S, Doi M, et al. (2011) Mutation-linked defective interdomain interactions within ryanodine receptor cause aberrant $Ca^{2+}$ release leading to catecholaminergic polymorphic ventricular tachycardia. *Circulation* **124:**682–694.
Tian C, Shao CH, Moore CJ, Kutty S, Walseth T, DeSouza C, and Bidasee KR (2011) Gain of function of cardiac ryanodine receptor in a rat model of type 1 diabetes. *Cardiovasc Res* **91:**300–309.
Uchida K (2000) Role of reactive aldehyde in cardiovascular diseases. *Free Radic Biol Med* **28:**1685–1696.
Vander Jagt DL (2008) Methylglyoxal, diabetes mellitus and diabetic complications. *Drug Metabol Drug Interact* **23:**93–124.
Vicentini J, Valentini J, Grotto D, Paniz C, Roehrs M, Brucker N, Charão MF, Moro AM, Tonello R, Moreira AP, et al. (2011) Association among microalbuminuria and oxidative stress biomarkers in patients with type 2 diabetes. *J Investig Med* **59:**649–654.
Watanabe H and Knollmann BC (2011) Mechanism underlying catecholaminergic polymorphic ventricular tachycardia and approaches to therapy. *J Electrocardiol* **44:**650–655.
Williams ME, Bolton WK, Khalifah RG, Degenhardt TP, Schotzinger RJ, and McGill JB (2007) Effects of pyridoxamine in combined phase 2 studies of patients with type 1 and type 2 diabetes and overt nephropathy. *Am J Nephrol* **27:**605–614.
Wong CM, Marcocci L, Liu L, and Suzuki YJ (2010) Cell signaling by protein carbonylation and decarbonylation. *Antioxid Redox Signal* **12:**393–404.
Yano M, Yamamoto T, Kobayashi S, and Matsuzaki M (2009) Role of ryanodine receptor as a $Ca^{2+}$ regulatory center in normal and failing hearts. *J Cardiol* **53:**1–7.
Yaras N, Ugur M, Ozdemir S, Gurdal H, Purali N, Lacampagne A, Vassort G, and Turan B (2005) Effects of diabetes on ryanodine receptor Ca release channel (RyR2) and $Ca^{2+}$ homeostasis in rat heart. *Diabetes* **54:**3082–3088.
Zhong Y, Ahmed S, Grupp IL, and Matlib MA (2001) Altered SR protein expression associated with contractile dysfunction in diabetic rat hearts. *Am J Physiol Heart Circ Physiol* **281:**H1137–H1147.
Zhou L, Aon MA, Liu T, and O'Rourke B (2011) Dynamic modulation of $Ca^{2+}$ sparks by mitochondrial oscillations in isolated guinea pig cardiomyocytes under oxidative stress. *J Mol Cell Cardiol* **51:**632–639.

**Address correspondence to:** Dr. Keshore R. Bidasee, Department of Pharmacology and Experimental Neuroscience, 985800 Nebraska Medical Center, Durham Research Center, DRC 3047, Omaha, NE 68198-5800. E-mail: kbidasee@unmc.edu